REPORT 1071

THEORETICAL SYMMETRIC SPAN LOADING DUE TO FLAP DEFLECTION FOR WINGS OF ARBITRARY PLAN FORM AT SUBSONIC SPEEDS [1]

By JOHN DEYOUNG

SUMMARY

A simplified lifting-surface theory is applied to the problem of evaluating span loading due to flap deflection for arbitrary wing plan forms. With the resulting procedure, the effects of flap deflection on the span loading and associated aerodynamic characteristics can be easily computed for any wing which is symmetrical about the root chord and which has a straight quarter-chord line over the wing semispan. The effects of compressibility and spanwise variation of section lift-curve slope are taken into account by the procedure.

For the case of straight-tapered wings, the load distribution and lift due to flap deflection are presented in chart form for a broad range of wing plan forms. Experimental values of flap effectiveness are compared with the values obtained from these charts for several wings. The comparison shows good agreement between theory and experiment.

The method presented can also be used to calculate the downwash in the vertical center of the wake of a wing which has arbitrary spanwise loading.

INTRODUCTION

Reference 1 presents a procedure which is based on simplified lifting-surface theory and which permits the rapid determination of the symmetric spanwise distribution of lift on wings having essentially arbitrary plan form. With reference 1, the symmetric spanwise loading can be found for any symmetric angle-of-attack distribution such as that due to spanwise continuous twist or camber. The method satisfies the boundary condition at only a finite number of spanwise points; thus, to insure accuracy for the loading obtained by this method, the angle-of-attack distribution must be continuous and must not vary excessively. If the angle-of-attack distribution is discontinuous, such as that due to partial wing-span flaps, or varies excessively, the boundary condition should be satisfied at sufficient points to insure a correct answer. This normally entails an excessive amount of labor, since the computations required increase approximately as the square of the number of points used.

An alternative procedure is to use a method which satisfies the boundary condition at only a few points where this boundary condition is adjusted so that at these points the calculated loading is identical with that which would be predicted by a method satisfying the boundary condition at all points. This specific boundary condition for the case of antisymmetrically deflected ailerons is developed in reference 2, which is based on the zero-aspect-ratio theory of reference 3. A similar development can determine the specific boundary condition for the case of symmetrically deflected flaps.

It is the purpose of the present report to determine the specific boundary condition and to provide simple methods for computing the aerodynamic characteristics for wings with symmetrically deflected flaps.

NOTATION

A	aspect ratio $\left(\frac{b^2}{S}\right)$
$a_{\nu n}$	coefficient depending on wing geometry and indicating the influence of symmetric loading at span station n on the downwash angle at span station ν
b	span of the wing measured perpendicular to the plane of symmetry, feet
c	wing chord,[2] feet
c_{av}	mean wing chord [2] $\left(\frac{S}{b}\right)$, feet
c_l	local lift coefficient $\left(\frac{\text{local lift}}{qc}\right)$
C_L	lift coefficient $\left(\frac{\text{total lift}}{qS}\right)$
C_{L_δ}	rate of change of lift coefficient with flap deflection, per radian
C_{L_α}	rate of change of lift coefficient with wing angle of attack, per radian
$\frac{c_l c}{C_L c_{av}}$	spanwise loading coefficient for unit lift coefficient $\left(\frac{2AG}{C_L}\right)$
d_ν	scale factor
e_{nk}	factors of loading interpolation function
G	spanwise loading coefficient or dimensionless circulation $\left(\frac{c_l c}{2b}\right)$ or $\left(\frac{\Gamma}{bV}\right)$
$\overline{\overline{G}}$	spanwise loading coefficient per radian of flap deflection $\left(\frac{G}{\delta_1}\right)$

[1] Supersedes NACA TN 2278, "Theoretical Symmetric Span Loading Due to Flap Deflection for Wings of Arbitrary Plan Form at Subsonic Speeds" by John DeYoung, 1951.

[2] Measured parallel to the plane of symmetry.

H_ν wing-chord distribution parameter (at span station ν) which includes the effects of compressibility and section lift-curve slope $\left[d_\nu\left(\frac{1}{\kappa_\nu}\right)\left(\frac{b}{c_\nu/\beta}\right)\right]$

h_n integration factors for spanwise loading due to flaps

M Mach number

m arbitrary number of span stations

q free-stream dynamic pressure, pounds per square foot

S wing area, square feet

V free-stream velocity, feet per second

w induced velocity, normal to the lifting surface, positive for downwash, feet per second

x longitudinal coordinate measured from the lateral plane through the quarter chord of the wing-root chord,[3] feet

y lateral coordinate measured from the wing root perpendicular to the plane of symmetry, feet

α wing angle of attack,[3] radians

α_ν section angle of attack at span station ν,[3] radians

$\frac{d\alpha}{d\delta}$ lift-effectiveness parameter[3] $\left(\frac{C_{L_\delta}}{C_{L_\alpha}}\right)$

β compressibility parameter $\sqrt{|1-M^2|}$

Γ circulation, feet squared per second

δ angle of deflection of flap,[3] radians

$\underline{\delta}$ angle of deflection of flap measured perpendicular to the hinge line, radians

η dimensionless lateral coordinate $\left(\frac{y}{b/2}\right)$

η_f dimensionless flap span on one wing panel, measured perpendicular to the plane of symmetry, from the wing root outboard for inboard flaps, and from the wing tip inboard for outboard flaps $\left(\frac{\text{flap span}}{b/2}\right)$

θ trigonometric spanwise coordinate defining the spanwise end of the flap, radians

κ_ν ratio of section lift-curve slope at span station ν to $\frac{2\pi}{\beta}$, both at the same Mach number [4]

Λ sweep angle of the wing quarter-chord line, positive for sweepback, degrees

Λ_β sweep parameter which includes the effects of compressibility $\left(\tan^{-1}\frac{\tan\Lambda}{\beta}\right)$, degrees

λ wing taper ratio $\left(\frac{\text{tip chord}}{\text{root chord}}\right)$

ξ dimensionless longitudinal coordinate $\left(\frac{x}{b/2}\right)$

ϕ trigonometric spanwise coordinate $(\cos^{-1}\eta)$, radians

[3] See footnote 2, page 1.
[4] See footnote 2, page 1.

SUBSCRIPTS

n integer pertaining to span station associated with the loading $\left(\eta=\cos\frac{n\pi}{m+1}\right)$

ν integer pertaining to span station associated with the downwash $\left(\eta=\cos\frac{\nu\pi}{m+1}\right)$

k half-integer pertaining to span station $\left(\eta=\cos\frac{k\pi}{m+1}\right)$

f pertaining to flaps

t wing tip,

r wing root

av average or mean

1 denoting full wing-chord flaps $\left(\frac{c_f}{c}=1\right)$

DEVELOPMENT OF METHOD

The simplified lifting-surface theory used herein replaces a lifting surface by a lifting vortex located at the wing quarter-chord line. The boundary condition specified for determining the vortex strength distribution is that, along the three-quarter-chord line of the wing, there shall be no flow through the lifting surface.

The mathematical method of solution and discussion of the limitations of the theory are given in detail in NACA Rep. 921, 1948 (reference 1). The same mathematical procedures and assumptions are used in the present report.

The mathematical solution for the determination of spanwise loading consists of satisfying the boundary condition that along the three-quarter-chord line of the wing there shall be no flow through the lifting surface. If the boundary condition (i. e., the spanwise twist along the three-quarter-chord line) can be approximated by a few terms of a mathematical series, then the "no-flow" condition need be satisfied exactly at only a few spanwise stations and the calculated loading can be expressed by a few terms of a mathematical series. Thus it has been found that satisfying the boundary conditions at four spanwise points enables accurate computation of the loading due to symmetric twist (reference 1), whereas only three spanwise points are required for accurate computation of the loading due to antisymmetric twist (reference 2). The distribution of spanwise twists in these two cases is such that at most a four and a three term trigonometric series, respectively, are needed to duplicate them.

For the case of irregular and discontinuous distribution of twist such as that required to simulate the span loading due to deflection of a partial-span flap, it becomes necessary to satisfy the boundary condition at a large number of points, particularly near the point of discontinuity, in order that sufficient accuracy will be insured. Since the computation labor increases approximately as the square of the number of points considered, the foregoing method becomes less practical. An alternate approach is to alter the boundary condition for the method involving few points at which the boundary condition is satisfied, so that at these points the loading is identical with that obtained by the method for which the boundary condition is satisfied at all points. This process is practical because the spanwise loading of

wings becomes independent of plan form as aspect ratio approaches zero (reference 3). Thus the solutions for the zero-aspect-ratio wing which satisfy the boundary condition at all points can be used to obtain the proper adjustment of the boundary condition for a method that satisfies the boundary condition at only a few points. With the altered boundary condition, the method satisfying conditions at only a few points will give accurate results for plan forms of very low aspect ratio, and should give good accuracy for wings of high aspect ratio since the alteration of the boundary condition can be kept small by proper choice of flap spans, and also since loading distribution is affected less by plan form than by the boundary condition. The mathematical procedure for determining the altered boundary conditions is developed in appendix A.

Although an altered boundary condition can be found for an arbitrary position of the point of discontinuity, the alteration can be made a minimum and of small order by locating the discontinuity at the mean position between two points at which the boundary condition is satisfied. With the point of discontinuity defined, the flap span becomes defined. The results for arbitrary flap spans are found by cross plots of results for the defined spans.

When the flap spans and corresponding twists (altered boundary conditions) have been determined, the method is applied in the same manner as that of reference 1. In this way, $(m+1)/2$ linear equations in terms of symmetric-loading distribution are obtained which satisfy the wing angle-of-attack conditions[5] at the three-quarter-chord line at m stations, where m is an arbitrary odd integer. The application in the present report is with $m=7$. The linear equations are represented by the summations

$$\alpha_\nu=\sum_{n=1}^{4} a_{\nu n}\, G_n, \qquad \nu=1,2,3,4 \tag{1}$$

where the integer subscripts ν and n pertain to span stations $\eta=\cos\ (\nu\pi/8)$ and $\cos\ (n\pi/8)$, respectively. To obtain the loading coefficients G_n from the simultaneous solution of equation (1), it remains only to evaluate the coefficients $a_{\nu n}$ (which depend on wing geometry, compressibility, and section lift-curve slope) and the spanwise variation of the symmetric angle of attack α_ν. The reader should note that with α_ν constant (spanwise) equation (1) represents additional loading, and that with α_ν varying symmetrically and continuously it represents basic loading (provided the net lift is zero).

EVALUATION OF $a_{\nu n}$

As shown in reference 1, $a_{\nu n}$ can be conveniently presented as a function of two parameters,[6] namely, a sweep parameter defined as $\Lambda_\beta=\tan^{-1}[(\tan\Lambda)/\beta]$ and a wing-chord distribution parameter H_ν defined by

$$H_\nu=d_\nu\left(\frac{1}{\kappa_\nu}\right)\left(\frac{b}{c_\nu/\beta}\right) \tag{2}$$

where

κ_ν ratio of experimental section lift-curve slope at span station ν to the theoretical value of $\frac{2\pi}{\beta}$, both at the same Mach number

c_ν wing chord at span station ν

d_ν scale factor which has the following values:

0.061 for $\nu=1$
.234 for $\nu=2$
.381 for $\nu=3$
.320 for $\nu=4$

Equation (2) can be written in an alternate form that gives H_ν in terms of wing geometry parameters that are more significant; thus

$$H_\nu=d_\nu\left(\frac{\beta A}{\kappa_{av}}\right)\frac{1}{(\kappa_\nu/\kappa_{av})(c_\nu/c_{av})} \tag{3}$$

where

κ_{av} ratio of average section lift-curve slope to $2\pi/\beta$, both at the same Mach number

$\frac{\kappa}{\kappa_{av}}$ spanwise distribution of section lift-curve slope for a given Mach number

$\frac{c_\nu}{c_{av}}$ spanwise distribution of the wing chord

$\frac{\beta A}{\kappa_{av}}$ aspect-ratio parameter

The term $1/(\kappa/\kappa_{av})(c_\nu/c_{av})$ of equation (3) gives the effective aerodynamic taper of a wing. The distribution of κ/κ_{av} may vary with Mach number, particularly at transonic speeds (e. g., due to spanwise variation of airfoil section). However, since this distribution contributes to taper effect, the primary change will be in the loading distribution rather than in gross load.

With H_ν determined from equation (2) or (3), the values of $a_{\nu n}$, 16 in all, can be found in figure 1 where $a_{\nu n}$ is given as a function of H_ν for various values of Λ_β.

For the case of straight-tapered wings with arbitrary section lift-curve-slope distribution for which the chord distribution is specified by taper ratio, evaluation of equation (3) is facilitated through the use of figure 2, which gives $\kappa_\nu H_\nu/\beta A$ for each of the four span stations as a function of taper ratio.

EVALUATION OF $\alpha_{\nu n}$

The symmetric angle-of-attack distributions most commonly encountered are those resulting from constant angle of attack, twist and camber, and the effective angle of attack due to flap deflection. The first two cases are the subjects of reference 1. The effective angle-of-attack distributions due to flap deflection are the subject of the present report.

To minimize the computations involved, it is convenient to consider the cases of inboard and outboard flaps independently. The inboard flaps are measured from the wing midspan outboard, and the outboard flaps are measured from the wing tip inboard. Three flap spans for inboard and outboard flaps are considered in appendix A and the equivalent angle-of-attack distribution for unit flap deflection α_ν/δ_1 for each case is listed in table A4. The values of α_ν/δ_1

[5] As discussed in reference 1, α_ν is not limited to small values but can be as large an angle as desired, provided separation does not occur.

[6] The effects of compressibility and section lift-curve slope are equivalent to a change in wing plan forms and can be taken into account by a proper adjustment of the $a_{\nu n}$ values.

given in table A4 are for $(c_f/c)=1$. The results can be easily modified for the case of $(c_f/c)<1$ as will be shown later. The case of full wing-span flaps is easily considered since this is the case of constant angle of attack which results in additional-type loading.

APPLICATION OF METHOD

For the cases of symmetric angle-of-attack distributions over a wing with flaps deflected, it is possible to form the set of simultaneous equations which are required for the solution of loading distribution for an arbitrary plan form. With the loading known, integration formulas can be given to determine aerodynamic coefficients.

The loading distribution G_n, determined from the solutions of the simultaneous equations, is a function of $a_{\nu n}$, which has been shown in a preceding section to be a function of wing geometry, compressibility, and section lift-curve slope. The aerodynamic coefficients are obtained by integrations of the laoding distribution and, therefore, will also be functions of wing geometry, compressibility, and section lift-curve-slope parameters.

In the following sections, application of the method to obtain the general solution for arbitrary spanwise distribution of wing chord is outlined and solutions are presented for the special case of wings having straight taper.

GENERAL SOLUTION

Simultaneous equations for the loading.—The $a_{\nu n}$ values to be substituted in the equations that follow are obtained from figure 1 and table 1[7] with values of H_ν given by equation (2) or (3).

1. *Deflected inboard flaps:* The flap spans measured from the wing midspan outboard are given by η_f. The set of simultaneous equations for symmetric spanwise loading due to deflection of any of the three following flap spans can be obtained from the appropriate set of the following equations:

Case	I	II	III	
η_f	0.195	0.556	0.831	
$\frac{\alpha_1}{\delta_1}$	−0.017	0.032	−0.041	$=a_{11}\bar{\bar{G}}_1+a_{12}\bar{\bar{G}}_2+a_{13}\bar{\bar{G}}_3+a_{14}\bar{\bar{G}}_4$
$\frac{\alpha_2}{\delta_1}$	.029	−.003	1.021	$=a_{21}\bar{\bar{G}}_1+a_{22}\bar{\bar{G}}_2+a_{23}\bar{\bar{G}}_3+a_{24}\bar{\bar{G}}_4$
$\frac{\alpha_3}{\delta_1}$	−.014	.994	.955	$=a_{31}\bar{\bar{G}}_1+a_{32}\bar{\bar{G}}_2+a_{33}\bar{\bar{G}}_3+a_{34}\bar{\bar{G}}_4$
$\frac{\alpha_4}{\delta_1}$	.988	.976	1.010	$=a_{41}\bar{\bar{G}}_1+a_{42}\bar{\bar{G}}_2+a_{43}\bar{\bar{G}}_3+a_{44}\bar{\bar{G}}_4$

(4)

where

$$\bar{\bar{G}}_n=G_n/\delta_1$$

For the case of $\eta_f=1$; α_ν/δ_1 is unity over the span of the wing (same condition as solution for additional loading).

2. *Deflected outboard flaps:* The flap spans measured from the wing tip inboard are given by η_f. The set of simultaneous equations for symmetric loading due to deflection of any of the three following flap spans can be obtained from the appropriate set of the following equations:

[7] Values of $a_{\nu n}$ beyond the scope of figure 1 and table I can be obtained from equation (B2), which gives the linear asymptotes of the $a_{\nu n}$ function.

Case	IV	V	VI	
η_f	0.169	0.444	0.805	
$\frac{\alpha_1}{\delta_1}$	1.041	0.968	1.017	$=a_{11}\bar{\bar{G}}_1+a_{12}\bar{\bar{G}}_2+a_{13}\bar{\bar{G}}_3+a_{14}\bar{\bar{G}}_4$
$\frac{\alpha_2}{\delta_1}$	−.021	1.003	.972	$=a_{21}\bar{\bar{G}}_1+a_{22}\bar{\bar{G}}_2+a_{23}\bar{\bar{G}}_3+a_{24}\bar{\bar{G}}_4$
$\frac{\alpha_3}{\delta_1}$	.045	.006	1.014	$=a_{31}\bar{\bar{G}}_1+a_{32}\bar{\bar{G}}_2+a_{33}\bar{\bar{G}}_3+a_{34}\bar{\bar{G}}_4$
$\frac{\alpha_4}{\delta_1}$	−.040	.024	.012	$=a_{41}\bar{\bar{G}}_1+a_{42}\bar{\bar{G}}_2+a_{43}\bar{\bar{G}}_3+a_{44}\bar{\bar{G}}_4$

(5)

where

$$\bar{\bar{G}}_n=G_n/\delta_1$$

For the case of $\eta_f=1$, $\alpha_\nu/\delta_1=1$.

Loading distribution.—The spanwise loading distributions can be determined for various flap configurations as follows:

1. *Full wing-chord flaps* $[(c_f/c)=1]$: The loading is zero at the wing tip and is determined at four other span stations of $\eta=\cos(n\pi/8)=0.924$, 0.707, 0.383, and 0 by solution of the appropriate set of simultaneous equations from the previous section. With equation (A9) and tables A6, A7, and A8, the loading can be interpolated at span stations $\eta=0.981$, 0.831, 0.556, and 0.195 for each of the flap spans considered. With these given points and the knowledge that the slope of the loading-distribution curve is theoretically infinite at the point of angle-of-attack discontinuity or flap spanwise end, the loading distribution can be faired. For flap spans other than those given, the loading distribution of flaps that are neither inboard nor outboard can be obtained from the concept that loadings are additive (discussed later).

2. *Constant fraction of wing-chord flaps* $[(c_f/c)=constant]$: The spanwise loading distribution is equal to the product of the loading distribution due to full wing-chord flaps and the lift-effectiveness parameter $d\alpha/d\delta$. The factor $d\alpha/d\delta$ is a function of the ratio of flap chord to wing chord c_f/c. Values of $d\alpha/d\delta$ are presented in figure 3, which is reproduced from figure 18 of reference 4. Although reference 4 from which figure 3 was taken limits the Mach number range to values less than 0.2, this limitation is believed to be too restrictive since linearized theory indicates that $d\alpha/d\delta$ is unaffected by compressibility for the two-dimensional wing. As indicated in reference 3, $d\alpha/d\delta$ is strongly affected by aspect ratio if the aspect ratio (or βA) becomes very small; however, comparisons with experiment indicate the values of $d\alpha/d\delta$ from figure 3 appear to be valid for $\beta A>2$. This limit to which $d\alpha/d\delta$ can be used will be considered further in the section Discussion when comparisons with experimental results are made.

3. *Arbitary spanwise distribution of flap chord* $[(c_f/c)=variable]$: The flap can be divided into several parts each having constant $d\alpha/d\delta$ and the load distribution due to each part determined. The total distribution is then the sum of these individual load distributions.

Lift coefficient.—The lift coefficients due to flap deflection for the same flap configurations previously discussed can be found as follows:

1. *Full wing-chord flaps* $[(c_f/c)=1]$: The spanwise loading due to flap deflection is, in general, so complicated that

numerical integration based on four spanwise values cannot be performed accurately with conventional integration formulas. However, in appendix A a special integration formula (which needs but four spanwise values) is developed which applies to the different flap spans. Equation (A6) can be written as

$$\frac{\beta C_{L_{\delta_1}}}{\kappa_{av}}=\left(\frac{\beta A}{\kappa_{av}}\right)(h_1\bar{\bar{G}}_1+h_2\bar{\bar{G}}_2+h_3\bar{\bar{G}}_3+h_4\bar{\bar{G}}_4) \tag{6}$$

where, for each of the cases of equations (4) and (5), the h_n values are given by

	Inboard flaps			Outboard flaps			Full span flaps
Case	I	II	III	IV	V	VI	
η_f	0.195	0.556	0.831	0.169	0.444	0.805	1.000
h_1	0.299	0.299	0.300	0.302	0.301	0.301	0.301
h_2	.544	.544	.555	.561	.556	.556	.555
h_3	.725	.725	.725	.734	.728	.726	.726
h_4	.392	.392	.392	.405	.395	.393	.393

2. Constant fraction of wing-chord flaps [$(c_f/c)=constant$]: The flap effectiveness is given by

$$\frac{\beta C_{L_\delta}}{\kappa_{av}}=\frac{d\alpha}{d\delta}\left(\frac{\beta C_{L_{\delta_1}}}{\kappa_{av}}\right) \tag{7}$$

3. Arbitrary spanwise distribution of flap chord [$(c_f/c)=variable$]: Flaps for which c_f/c varies spanwise on the wing can be considered as equivalent to a wing-twist distribution. The effective symmetric twist of the wing is given by

$$\alpha_v=\frac{d\alpha}{d\delta}\delta \tag{8}$$

where $d\alpha/d\delta$ is now a function of spanwise position. If equation (8) is a continuous distribution such that it can be plotted by specifying its value at four semispan points, then the wing can be considered to be twisted and solutions found directly as for basic loading.

When equation (8) is discontinuous, the angle of attack can be divided into spanwise steps of constant angle of attack and the total lift can be found by the summation of the lift due to each spanwise step. The lift of a spanwise step is obtained from a curve of lift coefficient $\frac{\beta C_{L_{\delta_1}}}{\kappa_{av}}$ as a function of the extent of flap span from the wing root outboard. Such a curve can be obtained from the solutions of equation (6). As previously indicated for $\eta_f=1$

$$\left(\frac{\beta C_{L_{\delta_1}}}{\kappa_{av}}\right)_{\eta_f=1}=\frac{\beta C_{L_\alpha}}{\kappa_{av}}$$

The lift coefficient due to the twist given by equation (8) can be obtained by a method other than the step method from the integral given by

$$\frac{\beta C_{L_\delta}}{\kappa_{av}}=\int_0^1\frac{d\alpha}{d\delta}\frac{d\left(\beta C_{L_{\delta_1}}/\kappa_{av}\right)}{d\eta}\,d\eta \tag{9}$$

which can be integrated numerically by taking the graphical slopes of $\beta C_{L_{\delta_1}}/\kappa_{av}$.

Spanwise center of pressure, induced drag, and pitching moment.—The integration formulas of loading due to flaps required to obtain spanwise center of pressure and induced drag are not developed here. However, the integration formulas given in reference 1 to obtain these characteristics can be used with acceptable accuracy for the case of loading due to flap deflection.

No rigorous procedure for determining pitching moments can be developed from this method. As noted in reference 1, however, a good approximation for a wing without flaps can be obtained if the wing sweep is large since moments due to shifts of spanwise load overshadow those due to shifts of chordwise load. Where the effect of flaps is to be considered, as in the present case, it appears unlikely that the shifts in chordwise loads can be safely neglected. Therefore an estimation of pitching moments due to flaps should not only include the moment due to spanwise load redistribution, which this method will give accurately from the longitudinal moment of the center of load, but also should include an estimation of the moment due to chordwise redistribution.

Additional considerations.—Several items pertaining to the usage of the method should be considered.

1. *Additive nature of loading and spanwise angle of attack:* The linear relation between angle of attack and loading distribution of equation (1) states that all loadings are additive if the respective angle-of-attack distributions are added.

Thus, the aerodynamic coefficients that result from the integration of the loading distribution are additive if they depend linearly on the loading distribution. Hence, lift coefficient, rolling-moment coefficient, and pitching moment are additive; whereas induced drag, spanwise center of pressure, and aerodynamic center are not.

The additive concept is very useful for the determination of loading due to flap deflection. The loading due to an arbitrary span flap having arbitrary position on the wing semispan is simply found by adding or subtracting known loadings due to flaps at other locations on the wing. For example, if the spanwise ends of the flaps are at the same span stations, then for full-chord flaps

$$\left.\begin{aligned} G_{\text{inboard}}&=G_{\eta_f=1}-G_{\text{outboard}}\\ (C_{L_\delta})_{\text{inboard}}&=C_{L_\alpha}-(C_{L_\delta})_{\text{outboard}}\\ \eta_{f_{\text{inboard}}}&=1-\eta_{f_{\text{outboard}}}\end{aligned}\right\} \tag{10}$$

2. *Differential flap angles:* The effect of a differential between flap angles can be taken into account by considering C_{L_δ} of each wing panel as having one-half the value of the symmetric case. The total wing lift is then the sum of the products of $C_{L_\delta}/2$ and the angle of deflection of each flap. Although the total wing lift can be found by this procedure, the loading distribution cannot be found exactly by the products of the symmetric G/δ and the deflection of each flap. However, the loading distribution so obtained will be sufficiently accurate for most purposes since this procedure neglects only the small change due to the induced effects of the difference in flap deflection on each opposite wing panel.

3. *Flap angles measured perpendicular to the hinge line:* The relationship between a flap angle measured in a plane

perpendicular to the flap hinge line and that measured in a plane parallel to the plane of symmetry is given by

$$\tan \underline{\delta}=\frac{\tan \delta}{\cos \Lambda_f} \tag{11}$$

where Λ_f is the sweep angle of the flap hinge line, and $\underline{\delta}$ is the angle measured perpendicular to the hinge line. Equation (11) can be inserted into any of the equations involving δ to put the equations in terms of $\underline{\delta}$.

For constant fraction of wing-chord flaps on straight-tapered wings, Λ_f is given by

$$\tan \Lambda_f=\tan \Lambda-\frac{4[(3/4)-(c_f/c)]}{A}\left(\frac{1-\lambda}{1+\lambda}\right) \tag{12}$$

SOLUTIONS FOR STRAIGHT-TAPERED WINGS

Charts of aerodynamic characteristics for straight-tapered wings can be presented in terms of parameters involving geometry, compressibility, and section lift-curve slope.[8] These charts provide a ready means of obtaining data directly.

Equation (4) has been used to evaluate the loading distribution $G/\delta_1=(1/\delta_1)\ (c_l c/2b)$ for a range of wing parameters and flap spans, and the results are plotted in figure 4. The loading presented in figure 4 gives the values due to full wing-chord flaps. For other flap configurations, the procedure given in the loading distribution section of the general solution can be used.

With the loading distribution determined from equation (4), the application of equation (6) provides lift coefficients due to flap deflection in the form $\beta C_{L_{\delta_1}}/\kappa_{a\beta}$ for several flap spans. In figure 5, these values are plotted against extent of flap span from the wing root outboard for a range of wing parameters.

As presented, figure 5 gives directly the lift due to full wing-chord inboard flaps for flap spans measured from the plane of symmetry outboard. The lift due to outboard flaps for flap spans measured from the wing tip inboard can be obtained from figure 5 by use of the relations of equation (10). For full wing-chord flaps located arbitrarily on the wing semispan, the lift can be obtained from figure 5 as indicated in the following example sketch:

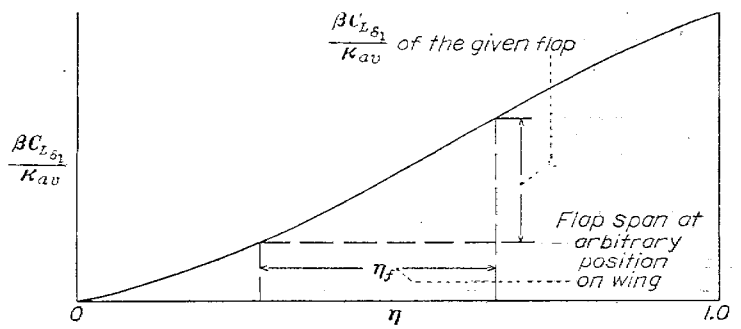

[8] Throughout the figures, $\kappa_{a\beta}$ is the constant spanwise-section lift-curve slope or the average of a small variation. For large spanwise variations of κ that follow the function given in equation (B5) developed in appendix B, the parameters $\beta A/\kappa_{a\beta}$ and λ can be replaced by the parameters $\frac{\beta A(1+\lambda)}{(\kappa_r+\kappa_t)}$ and $\frac{\kappa_t}{\kappa_r}\lambda$, respectively.

For large spanwise variations of κ that do not follow the curve of equation (B5), the simultaneous equations for the general solution can be solved for arbitrary distributions of κ. Values of H_ν can be obtained conveniently from figure 2.

With the full wing-chord values given above, the lift due to constant fraction of wing-chord and flaps of arbitrary spanwise chord distribution can be found through use of equations (7) and (9) with the $d\alpha/d\delta$ values of figure 3.

APPLICATION OF THE $a_{\nu n}$ COEFFICIENTS TO THE PREDICTION OF DOWNWASH FROM ARBITRARY WINGS

In the subject report and in reference 1, it is shown how various forms of symmetric loading can be found quickly through use of simplified lifting-surface theory and values of the $a_{\nu n}$ coefficients which are presented in graphical form. It can also be shown that if the symmetric load distribution is known, from any computational method or from experiment, then the same $a_{\nu n}$ coefficients can be used to find corresponding values of the downwash in the center of the downwash wake. It is the purpose of this section of the report to make available the method for computing downwash without attempting to explore the possibilities or limitations of the method. In view of the importance of being able to predict downwash, it is considered that inclusion of this material herein is justifiable although not directly related to the main purpose of the report. It is important to remember that the method can be used for any case of symmetric loading and is not restricted to that discussed in this report.

As noted previously, the $a_{\nu n}$ coefficients provide a very simple means of finding the downwash in the center of the downwash wake of the wing due to any symmetric spanwise loading distribution for any sweep angle. The downwash can be found at specific points in the region between the wing tips from near the quarter-chord line to an infinite distance downstream.

Equation (1) was derived (reference 1) to find the downwash at the effective three-quarter-chord line for which the distance downstream from the quarter-chord line is $\kappa(c/2)$. The general expression for the distance downstream from the quarter-chord line is

$$x-\beta y \tan \Lambda_\beta$$

where x is the longitudinal distance measured in the horizontal plane from the wing-root quarter-chord point to an arbitrary downwash point. Substituting this general expression in equation (2) gives

$$H_\nu=\frac{d_\nu}{(\xi/\beta)-\eta_\nu \tan \Lambda_\beta} \tag{13}$$

where

$$\xi=\frac{x}{b/2}$$

Equation (1) (for values of the parameters ξ/β, η_ν, and $\tan \Lambda_\beta$) gives the downwash angle as

$$\left(\frac{w}{V}\right)_{\frac{\xi}{\beta},\eta_\nu}=\sum_{n=1}^{4} a_{\nu n} G_n \tag{14}$$

where the $a_{\nu n}$ coefficients are obtained from figure 1 with the H_ν values given by equation (13).

It should be noticed that, because the chordwise loading is concentrated at the one-quarter-chord line, equation (13) is independent of aspect ratio and spanwise distribution of wing chord, while from equation (14) it can be seen that downwash depends on these wing geometric values only through the loading distribution G_n.

Equation (14) will give the downwash angle due to arbitrary symmetric loading distribution for all values of $\frac{\xi}{\beta}>\eta_\nu \tan \Lambda_\beta$. The downwash can be found for the specific span stations corresponding to $\nu=1, 2, 3, 4$, or $\eta_\nu=\cos\frac{\nu\pi}{8}=0.924$, 0.707, 0.383, and 0, respectively. If compressibility effects are included, the loading distribution must be that at the Mach number considered.

For convenience, equation (14) is rewritten such that downwash angle and loading distribution are in terms of unit lift coefficient. Then

$$\left(\frac{w/V}{\beta C_L/\kappa_{a_v}}\right)_{\frac{\xi}{\beta},\eta_\nu}=\frac{1}{2\left(\frac{\beta A}{\kappa_{a_v}}\right)}\sum_{n=1}^{4}a_{\nu n}\left(\frac{c_l c}{C_L c_{a_v}}\right)_n \qquad (15)$$

where $c_l c/C_L c_{a_v}$ is the span loading distribution for unit lift. Both $a_{\nu n}$ and $c_l c/C_L c_{a_v}$ are affected by compressibility, being functions of the parameters $\beta A/\kappa_{a_v}$ and Λ_β.

Equation (14) or (15) gives the downwash, in the vertical center of the wake, due to the integrated effect of the loading of a swept vortex and the trailing vortex sheet extending backwards to infinity. Any rolling of the trailing vortex sheet into two trails is neglected. Since either of the equations are for arbitrary loading distribution, the loading coefficient can be set equal to a constant to duplicate uniform loading and the downwash results obtained for the case of the trailing sheet rolled into two trails.

With $c_l c/C_L c_{a_v}=1$, equation (15) becomes

$$\left(\frac{w/V}{\beta C_L/\kappa_{a_v}}\right)_{\frac{\xi'}{\beta},\eta'}=\frac{\left(\frac{b}{b'}\right)}{2\left(\frac{\beta A}{\kappa_{a_v}}\right)}\sum_{n=1}^{4}a_{\nu n} \qquad (16)$$

where

$$\xi'=\frac{x}{b'/2}$$

$$\eta'=\frac{y}{b'/2}$$

and b' (as used in the past from line-theory concepts) is the span between the two trails given by the integrated loading divided by the loading at the middle of the wing, or

$$b'=\frac{b}{(c_l c/C_L c_{a_v})_{\eta=0}}$$

DISCUSSION

INFLUENCE OF WING GEOMETRY ON FLAP EFFECTIVENESS FOR STRAIGHT-TAPERED WINGS

To show the effect of wing geometry and compressibility on lift due to inboard flap deflection, the data of figure 5 have been cross-plotted and presented in figure 6. These effects are similar to those on wing lift-curve slope shown in reference 1. Figure 6 (a) compares the present theory with that of reference 3 and shows, as might be expected, that both theories give essentially the same results for $\frac{\beta A}{\kappa_{a_v}}<1$.

Figure 6 (b) shows the influence of taper ratio on flap effectiveness for swept wings. Figure 6 (c) gives the relative effects of the wing parameters of sweep, aspect ratio, and taper ratio.

Figure 7 shows comparative effects of inboard and outboard flaps on swept wings and shows the loss of flap effectiveness due to sweepback is less for inboard flaps. The relative effects indicated by figures 6 and 7 apply equally well for constant fraction of wing-chord flaps since the lift is only reduced by a constant spanwise factor $d\alpha/d\delta$.

LIMITATIONS OF THE $d\alpha/d\delta$ CONCEPT AND COMPRESSIBILITY CONSIDERATIONS

A minimum value of aspect ratio for which two-dimensional values of $d\alpha/d\delta$ can be used with accuracy has been determined for use with the subject report from principles of lifting-surface theory and from experiment. An analysis based on lifting-surface theory indicates that the $d\alpha/d\delta$ of a wing does not vary appreciably with aspect ratio until aspect ratio becomes less than approximately 2; for $A<2$, $d\alpha/d\delta$ increases rapidly with decreasing aspect ratio until at $A=0$, $d\alpha/d\delta=1$. The discussion of reference 2 concludes that only a lifting-surface theory that accounts for changes in chord loading due to flap deflection will give accurate loading predictions for low-aspect-ratio wings.

Low-speed experimental values of $d\alpha/d\delta$, from a 7- by 10-foot wind tunnel (reference 5), are plotted in figure 8 as a function of aspect ratio for an unswept and a swept-back wing. Figure 8 indicates the order of variation of $d\alpha/d\delta$ with aspect ratio.

The compressibility considerations in the present report are the same as those of reference 1, 2, or 3; namely, that compressibility can be taken into account by substituting for the geometric values of A, Λ, and b, the parameters βA, Λ_β, and βb, respectively.

From two-dimensional theory it can be shown that the parameter $d\alpha/d\delta$ is independent of Mach number. In the present report $d\alpha/d\delta$ is also considered independent of Mach number and, further, is considered independent of aspect ratio for $A>2$, as discussed earlier. However, from the linearized compressible-flow theory the aspect ratio becomes an effective aspect ratio given by βA which approaches zero as $M\rightarrow 1.0$. Thus the use of two-dimensional $d\alpha/d\delta$ is restricted to the Mach number range for which $\beta A>2$.

Figure 9 shows the flap-effectiveness comparison between theory and experiment for a subsonic range of speed for two wings. The theoretical values were obtained using $d\alpha/d\delta$ from figure 3 and assuming it independent of Mach number. The curves are terminated at the Mach number where $\beta A=2$. The parallelism of the theoretical and experimental curves of figure 9 indicates that $d\alpha/d\delta$ can be used with the assumption that it remains independent of Mach number to values of βA of the order of two.

In view of the foregoing discussion, it is believed that two-dimensional values of $d\alpha/d\delta$ can be considered independent of M as long as $\beta A\geqq 2$ in the application of the subject procedure.

COMPARISON OF THEORY WITH EXPERIMENT

Experimental values of flap effectiveness are compared with theoretically predicted values in a correlation diagram given by figure 10. Included are the results for a wide range of plan forms. Sketches of the plan forms and flaps are

drawn about the points of correlation. The theory makes use of the curve of figure 3 giving $d\alpha/d\delta$ for a sealed-gap flap over a range of deflection of $\pm 10°$. As seen in figure 10, the theory is in fair agreement with experiment.

In general, the theoretical values of figure 10 are too low and center approximately about the minus 10-percent line of the figure. A similar effect is shown in figures 8 and 9. This almost constant difference between the theoretical and experimental results is possibly due to the $d\alpha/d\delta$ values that were used in obtaining the theoretical results and which were obtained from the $-10°$ to $10°$ sealed-gap curve of figure 3.

The theoretical flap effectiveness of the low-aspect-ratio wings having partial-wing-chord flaps, given in figure 10, fall below the minus 10-percent line. Part of this discrepancy is presumably due to using two-dimensional values of $d\alpha/d\delta$ since these wings approached the lower limit of aspect ratio for which the $d\alpha/d\delta$ concept has been judged acceptable.

Comparison of experimental results with theory for a Mach number range is shown in figure 9. This figure shows that compressibility effects are accurately predicted up to Mach numbers corresponding to values of $\beta A=2$.

CONCLUDING REMARKS

The determination of symmetric loading due to flap deflection for arbitrary wings is shown to be obtained by the solution of four simultaneous equations. The coefficients of the simultaneous equations are presented in charts as functions of parameters that include wing geometry, compressibility, and section lift-curve slope. Integration formulas are given for the loading distribution. With these the flap effectiveness can be found.

For the special case of straight-tapered wings, the loading distributions and values of flap effectiveness are given in chart form for a range of wing plan forms. These charts indicate that the effects of plan form on the loading distribution and lift due to flap deflection are similar to that on additional loading.

On the basis of experimental comparisons, it is concluded that the method of the subject report can predict the flap effectiveness of wings at subsonic speeds with good accuracy.

AMES AERONAUTICAL LABORATORY,
NATIONAL ADVISORY COMMITTEE FOR AERONAUTICS,
MOFFETT FIELD, CALIF., *Sept. 22, 1950.*

APPENDIX A

DEVELOPMENT OF EQUATIONS FOR DETERMINATION OF SYMMETRIC SPAN LOADING AND LIFT DUE TO FLAP DEFLECTION

ALTERED BOUNDARY CONDITIONS FOR FLAP DEFLECTION

In the following development the flap chord is considered equal in length to the wing chord; thus a deflected flap results in a discontinuity in the spanwise distribution of angle of attack. Spanwise loading for a discontinuous distribution of angle of attack can be found through the simultaneous solution method of equation (1). The number of equations, however, must be greater than four to obtain accurate results and then the computation efforts become excessive. (Reference 1 gives the method for an arbitrary number of equations.) However, an alternate procedure, originally developed in reference 2, provides sufficient accuracy with a reasonable number of equations and this procedure is the basis of the following development.

The zero-aspect-ratio theory of reference 3 shows that for a given sweep angle, as aspect ratio approaches zero, spanwise loading becomes independent of plan form. Thus, the altered boundary conditions (see Development of Method) required for the present theory to give spanwise loading for given flap spans can be determined from the loading given by reference 3, which applies to all plan forms. These altered boundary conditions are obtained from equation (1) using the $a_{\nu n}$ values for zero aspect ratio and the loading distribution for zero-aspect-ratio wings given by reference 3 for given flap spans.

The zero-aspect-ratio values of $a_{\nu n}$ are given by figure 1 for $H_\nu=0$ or are given by the $B_{\nu n}$ coefficients of reference 1. These $a_{\nu n}$ coefficients are tabulated as follows:

TABLE A1

$a_{\nu n}$ (FOR $m=7$ AND $A=0$)

n \ ν	1	2	3	4
1	10.4524	−2.0720	0	−0.2242
2	−3.8284	5.6568	−1.8284	0
3	0	−2.3888	4.3296	−3.1548
4	−.2928	0	−1.7072	4.0000

With these $a_{\nu n}$ coefficients and equation (1), symmetric spanwise loading can be found for zero-aspect-ratio wings. As a comment on the accuracy of the simplified lifting-surface theory for determining additional loading with $m=7$, the solution of equation (1) with $A=0$, $a_{\nu n}$ values gave, to the accuracy of three decimal places, the elliptic loading distribution characteristic of zero-aspect-ratio wings.

The flap end is arbitrarily chosen for the present theory as the mean value of the spanwise trigonometric coordinates of the points at which the boundary condition is applied and which bracket the discontinuity or flap spanwise end. Thus for $m=7$, three flap spans can be defined for both inboard and outboard flaps. Let η_f be the flap span, and θ the spanwise point at the end of the flap, then

$$\eta_f=\cos\theta \text{ for inboard flaps}$$

$$\eta_f=1-\cos\theta \text{ for outboard flaps}$$

These flap spans are given in the following table:

TABLE A2

DEFINED FLAP SPANS

	Inboard			Outboard		
Case	I	II	III	IV	V	VI
θ	$\frac{7\pi}{16}$	$\frac{5\pi}{16}$	$\frac{3\pi}{16}$	$\frac{3\pi}{16}$	$\frac{5\pi}{16}$	$\frac{7\pi}{16}$
η_f	0.1951	0.5556	0.8315	0.1685	0.4444	0.8049

For the flap spans listed in table A2, the exact span loading distribution for zero-aspect ratio can be found from reference 3. With the a_{rn} values listed in table A1 and the exact values of G_1, G_2, G_3, and G_4 determined from reference 3, equation (1) gives the boundary condition or twist required for the present method to produce the loading distribution for each case listed in table A2, that is,

$$\left.\begin{aligned}
\frac{\alpha_1}{\delta_1}&=10.4524\,\frac{G_1}{\delta_1}-3.8284\,\frac{G_2}{\delta_1}-0.2928\,\frac{G_4}{\delta_1}\\
\frac{\alpha_2}{\delta_1}&=-2.0720\,\frac{G_1}{\delta_1}+5.6568\,\frac{G_2}{\delta_1}-2.3888\,\frac{G_3}{\delta_1}\\
\frac{\alpha_3}{\delta_1}&=-1.8284\,\frac{G_2}{\delta_1}+4.3296\,\frac{G_3}{\delta_1}-1.7022\,\frac{G_4}{\delta_1}\\
\frac{\alpha_4}{\delta_1}&=-0.2242\,\frac{G_1}{\delta_1}-3.1548\,\frac{G_3}{\delta_1}+4.0000\,\frac{G_4}{\delta_1}
\end{aligned}\right\} \quad \text{(A1)}$$

The spanwise loading distribution due to flap deflection is given by (reference 3):

Inboard flaps

$$\left.\begin{aligned}
\frac{G(\varphi)}{\delta_1}=\sin\varphi-\frac{1}{\pi}\Bigg[&2\theta\sin\varphi+(\cos\varphi-\cos\theta)\,ln\left|\frac{\sin\frac{\theta+\varphi}{2}}{\sin\frac{\theta-\varphi}{2}}\right|+\\
&(\cos\varphi+\cos\theta)\,ln\left|\frac{\cos\frac{\theta+\varphi}{2}}{\cos\frac{\theta-\varphi}{2}}\right|\Bigg]
\end{aligned}\right\} \quad \text{(A2)}$$

Outboard flaps

$$\left[\frac{G(\varphi)}{\delta_1}\right]_{\text{outboard}}=\sin\varphi-\left[\frac{G(\varphi)}{\delta_1}\right]_{\text{inboard}}$$

With equation (A2), the spanwise loading G_1, G_2, G_3, and G_4, at span stations $\varphi=\frac{\pi}{8}, \frac{\pi}{4}, \frac{3\pi}{8}$, and $\frac{\pi}{2}$ or $\eta=0.9239$, 0.7071, 0.3827, and 0 can be tabulated for each of the cases given in table A2 as follows:

TABLE A3

SPANWISE LOADING FOR $A=0$

$\frac{G_n}{\delta_1}$	Case I	II	III	IV	V	VI
$\frac{G_1}{\delta_1}$	0.0505	0.1524	0.2586	0.1241	0.2303	0.3322
$\frac{G_2}{\delta_1}$	.1106	.3467	.6432	.0639	.3604	.5965
$\frac{G_3}{\delta_1}$	.2062	.6903	.8714	.0525	.2336	.7177
$\frac{G_4}{\delta_1}$	.4125	.7970	.9618	.0382	.2030	.5875

The twist distribution required for each case is obtained with equation (A1) and table A3, and is summarized as follows:

TABLE A4

TWIST DISTRIBUTION, $\frac{\alpha_r}{\delta_1}$

	Inboard			Outboard		
Case	I	II	III	IV	V	VI
θ	$\frac{7\pi}{16}$	$\frac{5\pi}{16}$	$\frac{3\pi}{16}$	$\frac{3\pi}{16}$	$\frac{5\pi}{16}$	$\frac{7\pi}{16}$
$\overline{\eta}_f$	0.1951	0.5556	0.8315	0.1685	0.4444	0.8049
$\frac{\alpha_1}{\delta_1}$	−.0170	.0318	−.0414	1.0414	.9682	1.0170
$\frac{\alpha_2}{\delta_1}$	.0285	−.0034	1.0210	−.0210	1.0034	.9715
$\frac{\alpha_3}{\delta_1}$	−.0136	.9941	.9548	.0452	.0059	1.0136
$\frac{\alpha_4}{\delta_1}$	.9884	.9763	1.0404	−.0404	.0237	.0116

With the twist distribution given by table A4, equation (1) can be used to solve for spanwise loading due to flaps for any of the six cases and any aspect ratio.

LIFT DUE TO FLAPS

The loading distribution resulting from flap deflection is distorted to such an extent that the usual quadrature formulas are not sufficiently accurate to integrate the loading for $m=7$. However, the following development results in a method which will give the lift due to flaps as a function of the four loading coefficients:

Lift coefficient is given by the integral

$$C_L=A\int_{-1}^{1}G(\overline{n})d\overline{n}=A\int_0^{\pi}G(\varphi)\sin\varphi d\varphi$$

If it is assumed the loading series

$$G(\varphi)=\sum_{\mu_1=1}^{\infty}a_{\mu_1}\sin\mu_1\varphi$$

then

$$C_L=\frac{\pi A}{2}\,a_1 \quad \text{(A3)}$$

If the loading series is expanded for $\varphi=\frac{\pi}{8}, \frac{\pi}{4}, \frac{3\pi}{8}$, and $\frac{\pi}{2}$, and G_1, G_2, G_3, and G_4 are obtained in a series of a_{μ_1}'s, then multiplying each series through by the first coefficient of the series and summing the G's gives

$$a_1=\frac{1}{2}\left(0.3827\,G_1+0.7071\,G_2+0.9239\,G_3+\frac{G_4}{2}\right)+a_{15}-a_{17}+a_{31}-a_{33}+\ldots \quad \text{(A4)}$$

The high harmonic coefficients can be put as factors of the G_n. With equation (A4), the lift coefficient of equation (A3) becomes

$$\begin{aligned}
C_L=A\Bigg[&\frac{0.3827\,\pi}{4}\left(1+\frac{a_{15}-a_{17}+a_{31}-a_{33}}{1.5068\,G_1}\right)G_1+\\
&\frac{0.7071\pi}{4}\left(1+\frac{a_{15}-a_{17}+a_{31}-a_{33}}{1.5068\,G_2}\right)G_2+\\
&\frac{0.9239\pi}{4}\left(1+\frac{a_{15}-a_{17}+a_{31}-a_{33}}{1.5068\,G_3}\right)G_3+\\
&\frac{\pi}{4}\left(\frac{1}{2}+\frac{a_{15}-a_{17}+a_{31}-a_{33}}{1.5068\,G_4}\right)G_4\Bigg]
\end{aligned} \quad \text{(A5)}$$

If h_n is defined as the coefficients of G_n, then the lift coefficient is given by

$$C_L=A\ (h_1G_1+h_2G_2+h_3G_3+h_4G_4) \tag{A6}$$

Reference 3 also gives loading due to flaps in series form from which the ratio of $(a_{15}-a_{17}+a_{31}-a_{33})$ to G_n can be evaluated. It is expected that this ratio will not vary appreciably with aspect ratio. These high harmonic coefficients are small but are not negligible for loading due to flaps. The a_{μ_1} values from reference 3 are given by the following equations (for odd values of μ_1):

For inboard flaps

$$\left.\begin{aligned}&\mu_1=1\\&\qquad a_1=\frac{\delta_1}{\pi}(\pi-2\theta+\sin 2\theta)\\&\mu_1>1\\&\qquad a_{\mu_1}=\frac{4\delta_1}{\pi\mu_1(\mu_1^2-1)}(\mu_1\sin\theta\cos\mu_1\theta-\cos\theta\sin\mu_1\theta)\end{aligned}\right\}\tag{A7}$$

For outboard flaps (for the same θ)

$$\left.\begin{aligned}&\mu_1=1\\&\qquad (a_1)_{\text{outboard}}=\delta_1-(a_1)_{\text{inboard}}\\&\mu_1>1\\&\qquad (a_{\mu_1})_{\text{outboard}}=-(a_{\mu_1})_{\text{inboard}}\end{aligned}\right\}$$

With equations (A5) and (A7) and the values of table A3, the h_n values for each case can be tabulated:

TABLE A5

LOADING INTEGRATION FACTORS, h_n

Case	I	II	III	IV	V	VI
h_1	0.2991	0.2994	0.2999	0.3020	0.3014	0.3008
h_2	.5541	.5544	.5549	.5606	.5563	.5556
h_3	.7248	.7250	.7252	.7339	.7275	.7259
h_4	.3922	.3921	.3922	.4050	.3950	.3930

INTERPOLATION FUNCTION FOR SPANWISE LOADING DISTRIBUTION

The method of this report gives spanwise loading due to flap deflection at four span stations. Since the complete loading distribution is not sufficiently defined by these values, the values of loading at other span stations cannot be interpolated accurately by direct use of the interpolation equation and table of reference 1.

The direct use of the interpolation table of reference 1 can be obtained by converting the present loading due to flap deflection to a loading approximating additional loading distribution. The conversion factors are obtained from values of the zero-aspect-ratio theory and given by the ratio of equation (A2) to sin φ_n for each of the four given span stations. Define

$$R=\frac{(G/\delta_1)_{A=0}}{\sin\varphi} \tag{A8}$$

then, with table A3 and equation (A8), values of R_n have been computed and are tabulated for each of the flap span cases.

TABLE A6

R_n

		Inboard			Outboard		
Case		I	II	III	IV	V	VI
n	η_f / η	0.195	0.556	0.831	0.169	0.444	0.805
1	0.924	0.1318	0.3981	0.6757	0.3243	0.6019	0.8682
2	.707	.1564	.4903	.9036	.9041	.5097	.8436
3	.383	.2232	.7471	.9431	.5685	.2529	.7768
4	0	.4125	.7970	.9618	.0382	.2030	.5875

where, for $\eta_f=1$, $R_n=1$.

The interpolation table of reference 1 gives

TABLE A7

INTERPOLATION FACTORS e_{nk}

η_k	0.9808	0.8315	0.5556	0.1951
n / k	$\frac{1}{2}$	$\frac{3}{2}$	$\frac{5}{2}$	$\frac{7}{2}$
1	0.8657	0.4904	−0.0976	0.0229
2	−.3753	.7682	.5132	−.0746
3	.2778	−.3524	.7911	.4157
4	−.1275	.1503	−.2250	.6407

The interpolated loading at span station k is determined from the summation

$$\frac{G_k}{R_k}=\sum_{n=1}^{4}e_{nk}\left(\frac{G}{R}\right)_n \tag{A9}$$

where equations (A2) and (A8) provide values of R_k which are tabulated as follows:

TABLE A8

R_k

k	Case / η_k	I	II	III	IV	V	VI
$\frac{1}{2}$	0.981	0.1246	0.3826	0.6090	0.3911	0.6176	0.8754
$\frac{3}{2}$	.831	.1421	.4304	.8090	.1910	.5695	.8580
$\frac{5}{2}$	.556	.1799	.6253	.9314	.0685	.3746	.8201
$\frac{7}{2}$	.195	.3324	.7863	.9556	.0442	.2136	.6675

With the R_k values of table A8 and the loading ratios $\frac{G_k}{R_k}$ determined from equation (A9), the loading G_k can be found at span stations $k=\frac{1}{2}, \frac{3}{2}, \frac{5}{2}$, and $\frac{7}{2}$ ($\eta=0.981$, 0.831, 0.556 and 0.195, respectively).

APPENDIX B

AIDS TO THE METHOD

LINEAR ASYMPTOTE OF a_{rn}

For large values of H_r, the a_{rn} functions become linearly proportional to H_r (see, e. g., fig. 1). Since this linear charac-

teristic appears at relatively low values of H, the simple linear relation between a_{rn} and H, is quite useful.

The $L_{r\mu}$* function of appendix A of reference 1 is multiplied by b/c_r and the product is linearized with respect to b/c_r. The result gives

$$\left(\frac{b}{c_r}\right)L_{r\mu}^{*}=\begin{cases}-\dfrac{2}{\cos\Lambda}\left(\dfrac{b}{c_r}\right)+\left(\dfrac{1}{|\eta-\bar{\eta}|}-\dfrac{1}{\eta}\right)\sin\Lambda-\dfrac{2\bar{\eta}}{\eta^2-\bar{\eta}^2}+ \\ \qquad \dfrac{1}{2\eta}\tan\dfrac{\Lambda}{2}-\dfrac{\sqrt{1+\left(\dfrac{\eta-\bar{\eta}}{\eta+\bar{\eta}}\tan\Lambda\right)^2}-1}{2\eta\tan\Lambda} & \text{for } \bar{\eta}>\eta \\ =\left(\dfrac{1}{|\eta-\bar{\eta}|}-\dfrac{1}{\eta}\right)\sin\Lambda-\dfrac{2\bar{\eta}}{\eta^2-\bar{\eta}^2}+\dfrac{1}{2\eta}\tan\dfrac{\Lambda}{2}- \\ \qquad \dfrac{\sqrt{1+\left(\dfrac{\eta-\bar{\eta}}{\eta+\bar{\eta}}\tan\Lambda\right)^2}-1}{2\eta\tan\Lambda}\cdots & \text{for } \bar{\eta}<\eta \\ =-\left(\dfrac{1}{\cos\Lambda}-\tan\Lambda\right)\left(\dfrac{b}{c_r}\right)-\dfrac{\sin\Lambda}{\eta}+ \\ \qquad \dfrac{1}{2\eta}+\dfrac{1}{2\eta}\tan\dfrac{\Lambda}{2}\cdots & \text{for } \bar{\eta}=\eta \\ =-2\left(\dfrac{1}{\cos\Lambda}+\tan\Lambda\right)\left(\dfrac{b}{c_r}\right)+\dfrac{2}{\bar{\eta}}(1+\sin\Lambda)\cdots & \text{for } \eta=0\end{cases} \tag{B1}$$

With the values of equation (B1) substituted into equation (A37) of reference 1, the values of a_{rn} for arbitrary sweep angle and for high values of H, are obtained. For $m=7$, the following equation (B2) gives values for a_{rn} as

$$\begin{aligned}
a_{11}&=\left(\frac{3.913}{\cos\Lambda}+1.452\tan\Lambda\right)H_1+7.915-1.751\sin\Lambda- \\
&\quad 0.003\tan\frac{\Lambda}{2}+0.088\left(\frac{\sqrt{1+0.0016\tan^2\Lambda}-1}{\tan\Lambda}\right)- \\
&\quad 0.052\left(\frac{\sqrt{1+0.0177\tan^2\Lambda}-1}{\tan\Lambda}\right)+ \\
&\quad 0.014\left(\frac{\sqrt{1+0.1716\tan^2\Lambda}-1}{\tan\Lambda}\right) \\
a_{12}&=\left(\frac{0.892}{\cos\Lambda}-3.793\tan\Lambda\right)H_1-3.100+1.610\sin\Lambda+ \\
&\quad 0.008\tan\frac{\Lambda}{2}-0.048\left(\frac{\sqrt{1+0.0016\tan^2\Lambda}-1}{\tan\Lambda}\right)- \\
&\quad 0.034\left(\frac{\sqrt{1+0.0177\tan^2\Lambda}-1}{\tan\Lambda}\right)- \\
&\quad 0.052\left(\frac{\sqrt{1+0.1716\tan^2\Lambda}-1}{\tan\Lambda}\right) \\
a_{13}&=\left(\frac{-0.256}{\cos\Lambda}+2.476\tan\Lambda\right)H_1-0.014-1.727\sin\Lambda- \\
&\quad 0.032\tan\frac{\Lambda}{2}+0.037\left(\frac{\sqrt{1+0.0016\tan^2\Lambda}-1}{\tan\Lambda}\right)+ \\
&\quad 0.125\left(\frac{\sqrt{1+0.0177\tan^2\Lambda}-1}{\tan\Lambda}\right)- \\
&\quad 0.048\left(\frac{\sqrt{1+0.1716\tan^2\Lambda}-1}{\tan\Lambda}\right)
\end{aligned} \tag{B2}$$

$$\begin{aligned}
a_{14}&=\left(\frac{0.084}{\cos\Lambda}-1.100\tan\Lambda\right)H_1-0.043+0.637\sin\Lambda- \\
&\quad 0.060\tan\frac{\Lambda}{2}-0.017\left(\frac{\sqrt{1+0.0016\tan^2\Lambda}-1}{\tan\Lambda}\right)- \\
&\quad 0.048\left(\frac{\sqrt{1+0.0177\tan^2\Lambda}-1}{\tan\Lambda}\right)+ \\
&\quad 0.088\left(\frac{\sqrt{1+0.1716\tan^2\Lambda}-1}{\tan\Lambda}\right) \\
a_{21}&=\left(\frac{0.231}{\cos\Lambda}+0.408\tan\Lambda\right)H_2-2.140-0.223\sin\Lambda- \\
&\quad 0.004\tan\frac{\Lambda}{2}-0.063\left(\frac{\sqrt{1+0.0177\tan^2\Lambda}-1}{\tan\Lambda}\right)+ \\
&\quad 0.116\left(\frac{\sqrt{1+0.0294\tan^2\Lambda}-1}{\tan\Lambda}\right)+ \\
&\quad 0.018\left(\frac{\sqrt{1+0.0886\tan^2\Lambda}-1}{\tan\Lambda}\right) \\
a_{22}&=\left(\frac{0.951}{\cos\Lambda}+0.267\tan\Lambda\right)H_2+4.640-0.491\sin\Lambda+ \\
&\quad 0.011\tan\frac{\Lambda}{2}+0.163\left(\frac{\sqrt{1+0.0177\tan^2\Lambda}-1}{\tan\Lambda}\right)- \\
&\quad 0.063\left(\frac{\sqrt{1+0.0294\tan^2\Lambda}-1}{\tan\Lambda}\right)- \\
&\quad 0.068\left(\frac{\sqrt{1+0.0886\tan^2\Lambda}-1}{\tan\Lambda}\right)
\end{aligned} \tag{B2}$$

$$\begin{aligned}
a_{23}&=\left(\frac{0.275}{\cos\Lambda}-0.986\tan\Lambda\right)H_2-2.226+0.821\sin\Lambda- \\
&\quad 0.042\tan\frac{\Lambda}{2}-0.107\left(\frac{\sqrt{1+0.0177\tan^2\Lambda}-1}{\tan\Lambda}\right)+ \\
&\quad 0.048\left(\frac{\sqrt{1+0.0294\tan^2\Lambda}-1}{\tan\Lambda}\right)- \\
&\quad 0.063\left(\frac{\sqrt{1+0.0886\tan^2\Lambda}-1}{\tan\Lambda}\right) \\
a_{24}&=\left(-\frac{0.067}{\cos\Lambda}+0.377\tan\Lambda\right)H_2+0.188-0.551\sin\Lambda- \\
&\quad 0.079\tan\frac{\Lambda}{2}+0.048\left(\frac{\sqrt{1+0.0177\tan^2\Lambda}-1}{\tan\Lambda}\right)- \\
&\quad 0.022\left(\frac{\sqrt{1+0.0294\tan^2\Lambda}-1}{\tan\Lambda}\right)+ \\
&\quad 0.116\left(\frac{\sqrt{1+0.0886\tan^2\Lambda}-1}{\tan\Lambda}\right) \\
a_{31}&=\left(-\frac{0.041}{\cos\Lambda}-0.068\tan\Lambda\right)H_3+0.197+0.207\sin\Lambda- \\
&\quad 0.007\tan\frac{\Lambda}{2}-0.116\left(\frac{\sqrt{1+0.1716\tan^2\Lambda}-1}{\tan\Lambda}\right)- \\
&\quad 0.125\left(\frac{\sqrt{1+0.0886\tan^2\Lambda}-1}{\tan\Lambda}\right)+ \\
&\quad 0.2134\left(\frac{\sqrt{1+0.1993\tan^2\Lambda}-1}{\tan\Lambda}\right)
\end{aligned} \tag{B2}$$

$$
\begin{aligned}
a_{32}&=\left(\frac{0.170}{\cos\Lambda}+0.251\tan\Lambda\right)H_3-1.850-0.132\sin\Lambda+\\
&\quad 0.020\tan\frac{\Lambda}{2}+0.302\left(\frac{\sqrt{1+0.1716\tan^2\Lambda}-1}{\tan\Lambda}\right)-\\
&\quad 0.082\left(\frac{\sqrt{1+0.0886\tan^2\Lambda}-1}{\tan\Lambda}\right)-\\
&\quad 0.116\left(\frac{\sqrt{1+0.1993\tan\Lambda}-1}{\tan\Lambda}\right)\\
a_{33}&=\left(\frac{0.543}{\cos\Lambda}+0.232\tan\Lambda\right)H_3+4.272-0.388\sin\Lambda-\\
&\quad 0.078\tan\frac{\Lambda}{2}-0.197\left(\frac{\sqrt{1+0.1716\tan^2\Lambda}-1}{\tan\Lambda}\right)+\\
&\quad 0.302\left(\frac{\sqrt{1+0.0886\tan^2\Lambda}-1}{\tan\Lambda}\right)+\\
&\quad 0.088\left(\frac{\sqrt{1+0.1993\tan^2\Lambda}-1}{\tan\Lambda}\right)\\
a_{34}&=\left(\frac{0.156}{\cos\Lambda}-0.428\tan\Lambda\right)H_3-1.666+0.489\sin\Lambda-\\
&\quad 0.145\tan\frac{\Lambda}{2}+0.088\left(\frac{\sqrt{1+0.1716\tan^2\Lambda}-1}{\tan\Lambda}\right)-\\
&\quad 0.116\left(\frac{\sqrt{1+0.0886\tan^2\Lambda}-1}{\tan\Lambda}\right)-\\
&\quad 0.041\left(\frac{\sqrt{1+0.1993\tan^2\Lambda}-1}{\tan\Lambda}\right)\\
a_{41}&=0.032\left(\frac{1}{\cos\Lambda}+\tan\Lambda\right)H_4-0.224\\
a_{42}&=-0.097\left(\frac{1}{\cos\Lambda}+\tan\Lambda\right)H_4+0.354\,(1+\sin\Lambda)\\
a_{43}&=0.371\left(\frac{1}{\cos\Lambda}+\tan\Lambda\right)H_4-3.155\\
a_{44}&=0.696\left(\frac{1}{\cos\Lambda}+\tan\Lambda\right)H_4+3.313-0.687\sin\Lambda
\end{aligned}
\qquad \text{(B2)}
$$

LINEAR SPANWISE DISTRIBUTION OF $(\kappa c)_\nu/(\kappa c)_{\nu=0}$

Equation (3) can be manipulated into a function of various parameters involving distributions of wing chord and section lift-curve slope. One procedure is as follows: With the condition that the product of section lift-curve slope and wing chord varies linearly spanwise, then

$$(\kappa c)=\frac{2b}{A_\kappa(1+\kappa_t\lambda/\kappa_r)}\left[1-\eta_\nu\left(1-\frac{\kappa_t}{\kappa_r}\lambda\right)\right] \qquad \text{(B3)}$$

and equation (3) becomes

$$H_\nu=d_\nu(\beta A_\kappa)\frac{1+\kappa_t\lambda/\kappa_r}{2[1-\eta_\nu(1-\kappa_t\lambda/\kappa_r)]}$$

where A_κ is the aspect ratio based on a wing chord equal to (κc). Equation (B3) is reduced to terms of two parameters, A_κ and $(\kappa_t/\kappa_r)\lambda$. Expressions of A_κ in terms of aspect ratio for straight-tapered wings, and the distribution of section lift-curve slope can be found.

For straight-tapered wings

$$A=\frac{2b}{c_r(1+\lambda)}$$

and since (κc) is linear

$$A_\kappa=\frac{2b}{\kappa_r c_r[1+(\kappa_t/\kappa_r)\lambda]}$$

then

$$A_\kappa=\frac{A(1+\lambda)}{\kappa_r+\kappa_t\lambda}$$

and equation (B3) becomes

$$H_\nu=d_\nu\left[\frac{\beta A(1+\lambda)}{(\kappa_r+\kappa_t\lambda)}\right]\frac{1+(\kappa_t/\kappa_r)\lambda}{2\{1-\eta_\nu[1-(\kappa_t/\kappa_r)\lambda]\}} \qquad \text{(B4)}$$

The distribution of κ for straight-tapered wings is given by

$$\kappa_\nu=\frac{(\kappa c)_\nu}{c_\nu}=\kappa_r\frac{1-\eta_\nu[1-(\kappa_t/\kappa_r)\lambda]}{1-\eta_\nu(1-\lambda)} \qquad \text{(B5)}$$

Equation (B4) is in terms of the two parameters $\left[\frac{\beta A(1+\lambda)}{(\kappa_r+\kappa_t\lambda)}\right]$ and $(\kappa_t/\kappa_r)\lambda$. Solutions for spanwise loading in terms of these two parameters and Λ_β are valid for the distributions of section lift-curve slope given by equation (B5). Equation (B5) indicates that at $\lambda=1$, κ_ν is a linear function and at $\lambda=0$, κ_ν is a constant. For values of λ between 0 and 1, κ_ν is a curve in the region between the linear function and a constant.

Equation (B4) is represented in graphical form by figure 2 but with the ordinate replaced by the parameter $\frac{H_\nu}{\beta A(1+\lambda)/(\kappa_r+\kappa_t\lambda)}$ and the abscissa by $(\kappa_t/\kappa_r)\lambda$.

In summary, for straight-tapered wings having a linear distribution $(\kappa c)_\nu$, the loading and associated aerodynamic characteristics can be presented in terms of the parameters Λ_β, $\frac{\beta A(1+\lambda)}{\kappa_r+\kappa_t\lambda}$, and $(\kappa_t/\kappa_r)\lambda$.

REFERENCES

1. DeYoung, John, and Harper, Charles W.: Theoretical Symmetric Span Loading at Subsonic Speeds for Wings Having Arbitrary Plan Form. NACA Rep. 921, 1948.
2. DeYoung, John: Theoretical Antisymmetric Span Loading for Wings of Arbitrary Plan Form at Subsonic Speeds. NACA TN 2140, 1950.
3. DeYoung, John: Spanwise Loading for Wings and Control Surfaces of Low Aspect Ratio. NACA TN 2011, 1950.
4. Toll, Thomas A.: Summary of Lateral-Control Research. NACA Rep. 868, 1947.
5. Dods, Jules B., Jr.: Estimation of Low-Speed Lift and Hinge Moment Parameters for Full-Span Trailing-Edge Flaps on Lifting Surfaces With and Without Sweepback. NACA TN 2288, 1951

TABLE I.—SYMMETRIC INFLUENCE COEFFICIENTS, a_{rs} BEYOND THE SCOPE OF FIGURE 1

a_{11}

H_1 \ Λ_β	−45	−40	−20	0	20	40	50	60	70	75
0.8	-----	-----	-----	-----	-----	-----	------	------	18.60	22.67
1.0	-----	-----	-----	-----	-----	-----	------	------	21.66	26.78
1.2	-----	-----	-----	-----	-----	-----	16.26	18.95	24.72	30.88
1.6	15.86	-----	-----	-----	-----	17.20	19.26	22.96	30.84	39.09
2.0	17.44	17.00	16.08	16.19	16.94	19.54	22.26	27.14	36.90	------
2.4	-----	18.52	17.40	17.66	18.54	21.85	25.26	31.27	------	------
2.8	-----	-----	18.72	19.18	20.14	24.22	28.26	------	------	------
3.2	-----	-----	20.04	20.72	21.74	26.56	31.26	------	------	------
3.6	-----	-----	21.36	22.26	23.34	28.90	34.26	------	------	------
4.0	-----	-----	-----	23.80	24.94	31.24	------	------	------	------

a_{13}

H_1 \ Λ_β	−45	−40	−20		20	40	50	60	70	75
0.6	−1.32	−2.02	-----	-----	-----	-----	------	------	−6.35	−8.00
.8	−.30	−1.52	−2.05	-----	-----	-----	------	------	−8.07	−10.14
1.0	.72	−1.02	−1.55	-----	-----	-----	------	−6.60	−9.79	−12.28
1.2	1.72	−.52	−1.05	-----	-----	-----	------	−7.73	−11.51	−14.42
1.6	3.76	.48	−.05	-----	-----	-----	−7.03	−9.41	−14.95	−18.70
2.0	5.82	1.48	.95	-----	-----	-----	−8.29	−11.32	−18.39	------
2.4	-----	2.48	1.95	-----	-----	−6.95	−9.55	−13.23	------	------
2.8	-----	-----	2.95	-----	-----	−7.71	−10.81	------	------	------
3.2	-----	-----	3.95	-----	-----	−8.47	−12.07	------	------	------
3.6	-----	-----	4.95	-----	-----	−9.23	−13.23	------	------	------
4.0	-----	-----	-----	-----	-----	−9.97	------	------	------	------

a_{12}

H_1 \ Λ_β	−45	−40	−20	0	20	40	50	60	70	75
0.8	−1.03	-----	-----	-----	-----	-----	------	------	3.23	4.91
1.0	−1.59	−1.26	-----	-----	-----	-----	------	------	4.37	6.55
1.2	−2.20	−1.72	-----	-----	-----	-----	------	------	5.51	8.20
1.6	−3.33	−2.64	−1.23	-----	-----	-----	------	4.54	7.79	11.50
2.0	−4.39	−3.56	−1.71	-----	-----	-----	------	6.04	10.07	------
2.4	-----	−4.48	−2.19	-----	-----	-----	4.73	7.55	------	------
2.8	-----	-----	−2.67	-----	-----	-----	5.71	------	------	------
3.2	-----	-----	−3.15	-----	-----	4.45	6.69	------	------	------
3.6	-----	-----	−3.63	-----	-----	5.15	7.67	------	------	------
4.0	-----	-----	-----	-----	-----	6.30	------	------	------	------

a_{14}

H_1 \ Λ_β	−45	−40	−20	0	20	40	50	60	70	75
1.0	-----	-----	-----	-----	-----	-----	------	------	------	−3.31
1.2	-----	-----	-----	-----	-----	-----	------	------	------	−4.01
1.6	1.45	1.17	-----	-----	-----	-----	------	------	−4.06	−5.61
2.0	1.93	1.59	-----	-----	-----	-----	------	------	−4.67	------
2.4	-----	2.01	-----	-----	-----	-----	------	------	−5.28	------
2.8	-----	-----	1.06	-----	-----	-----	------	------	−5.89	------
3.2	-----	-----	1.27	-----	-----	-----	------	------	------	------

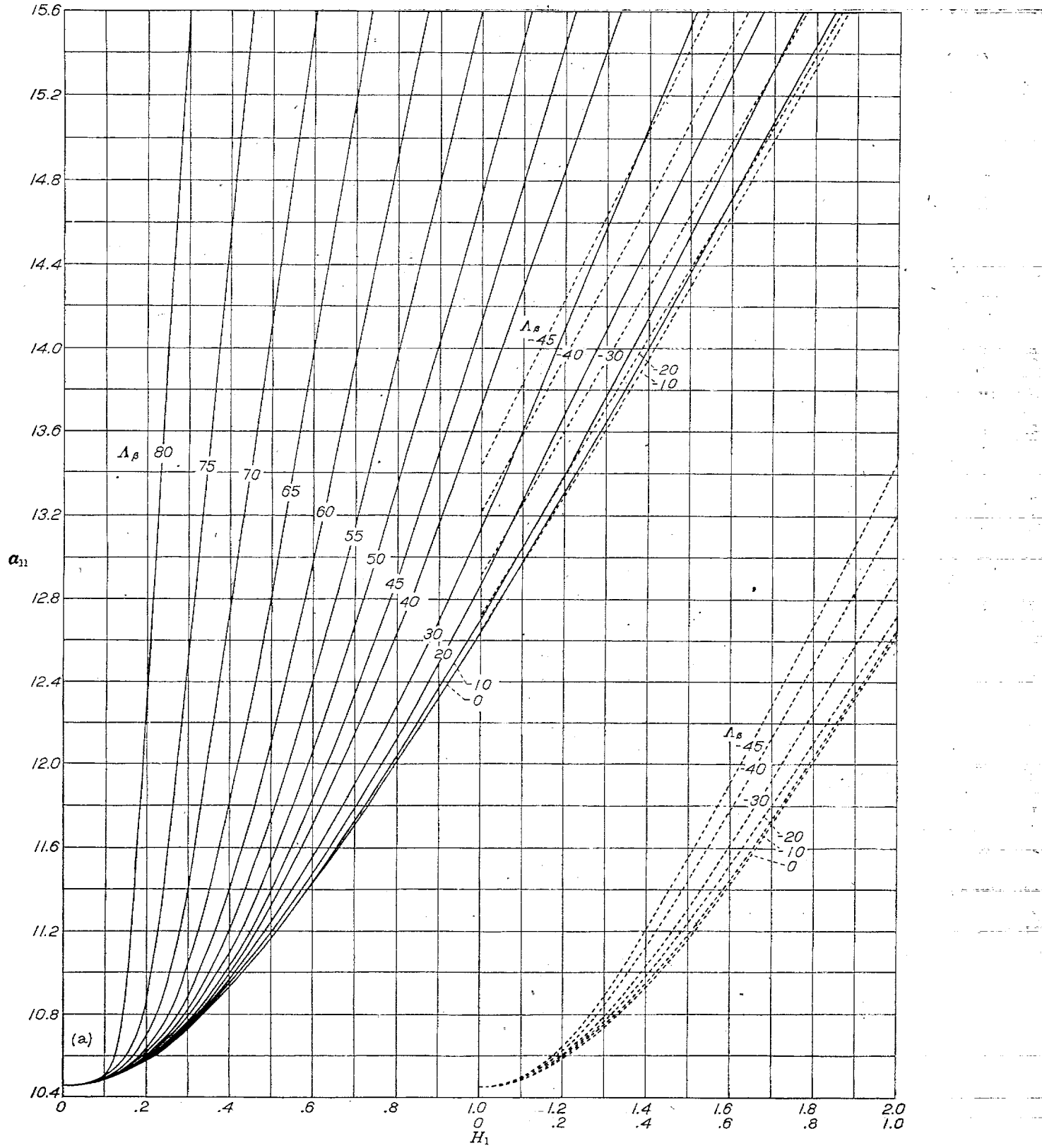

FIGURE 1.—Influence coefficients, a_{rs}, for symmetric spanwise loading plotted as a function of the wing-chord-distribution parameter, H_1, for values of the sweep parameter, Λ_β, degrees.
(a) $\nu=1$, $n=1$, $d_1=0.061$.

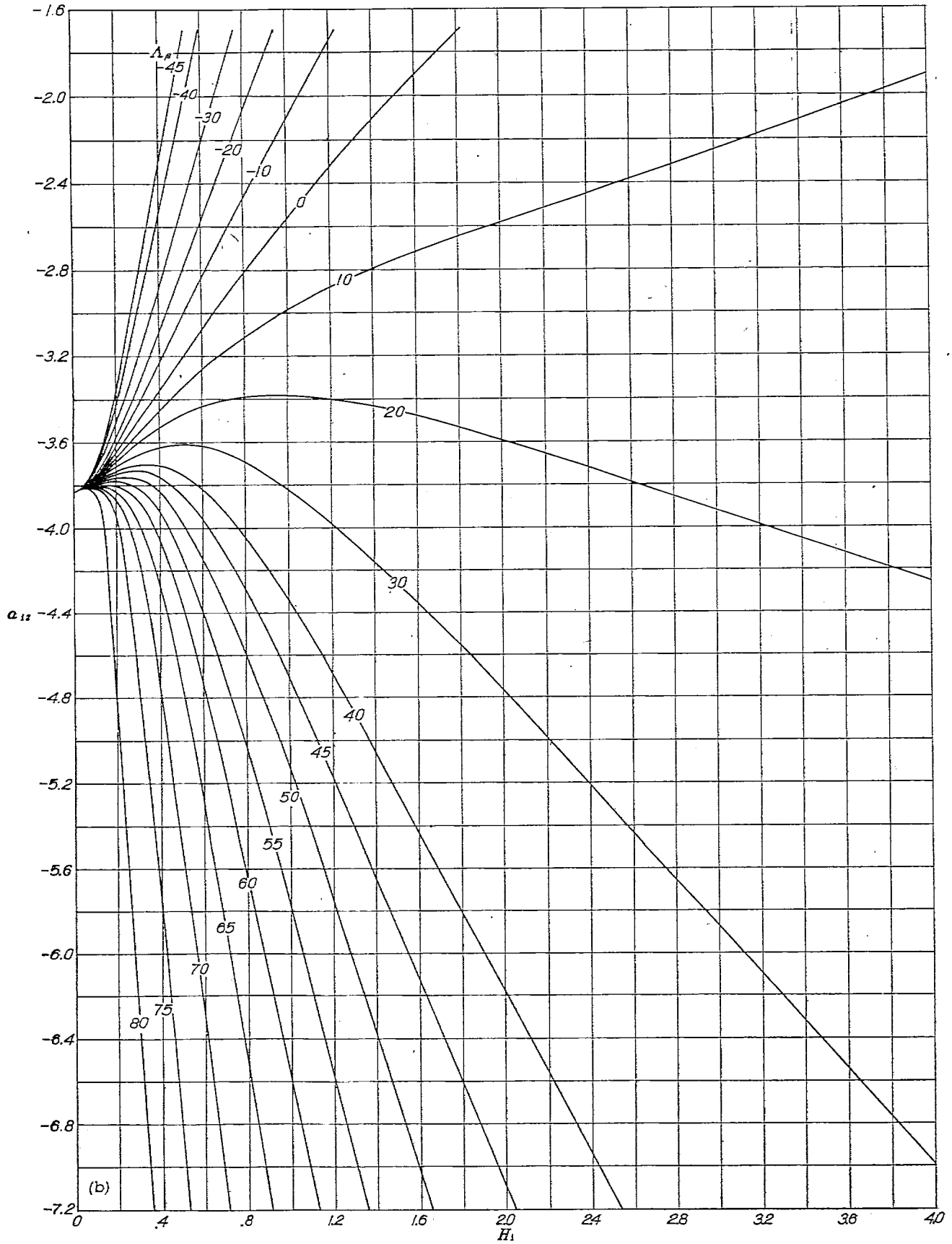

FIGURE 1.—Continued. (b) $\nu=1$, $n=2$, $d_1=0.061$.

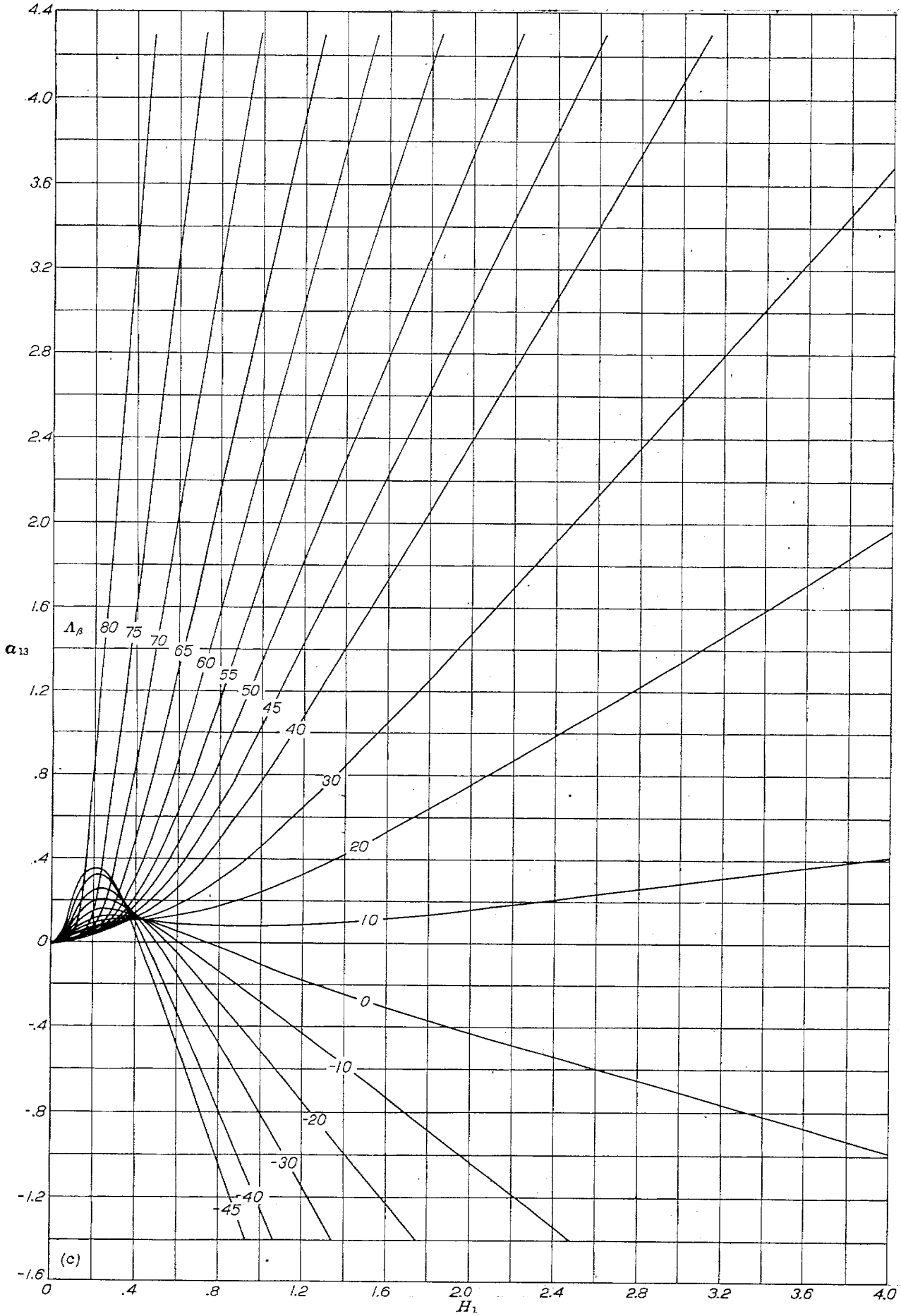

FIGURE 1.—Continued. (c) $\nu=1$, $n=3$, $d_1=0.061$.

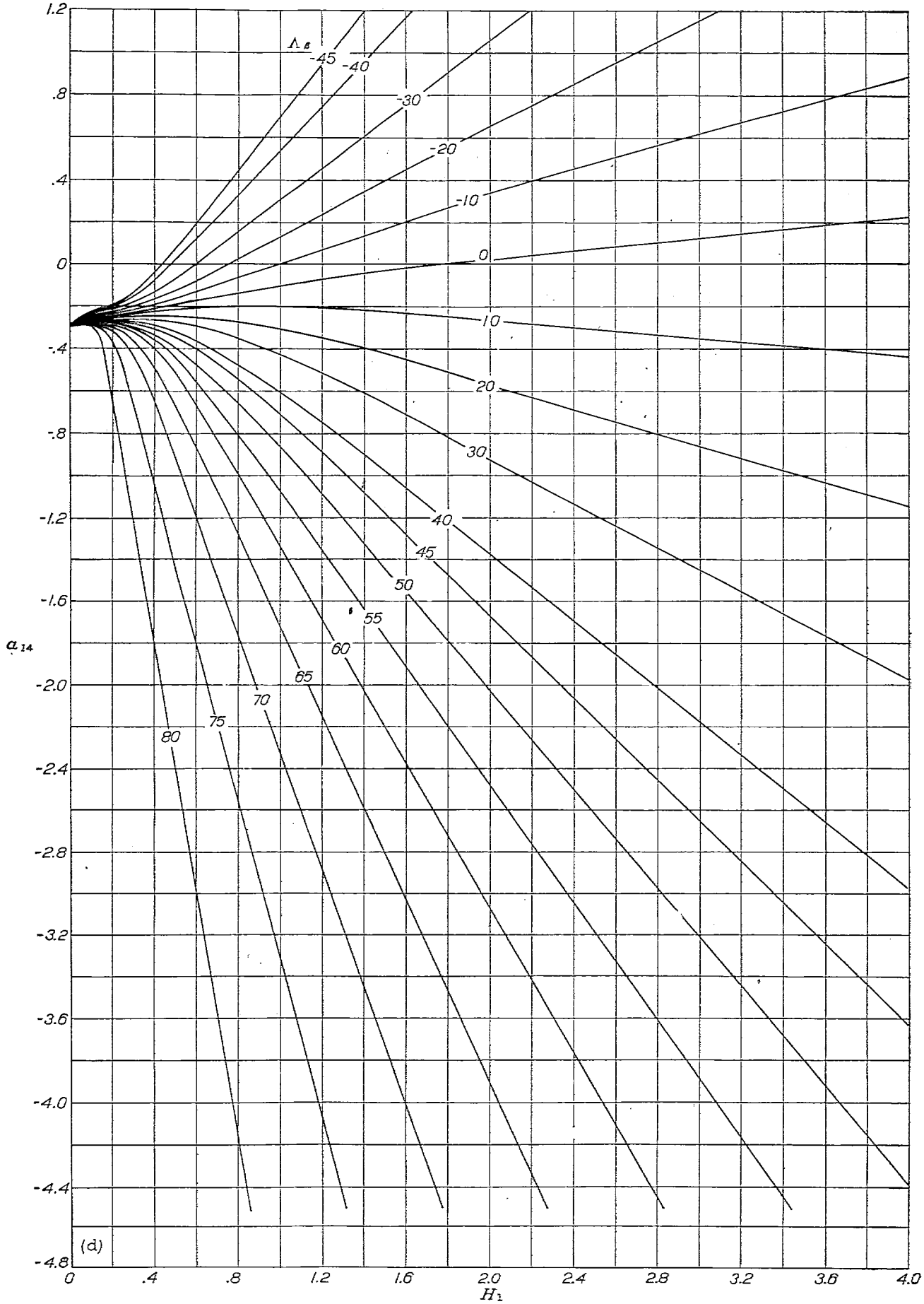

FIGURE 1.—Continued. (d) $\nu=1$, $n=4$, $d_1=0.061$.

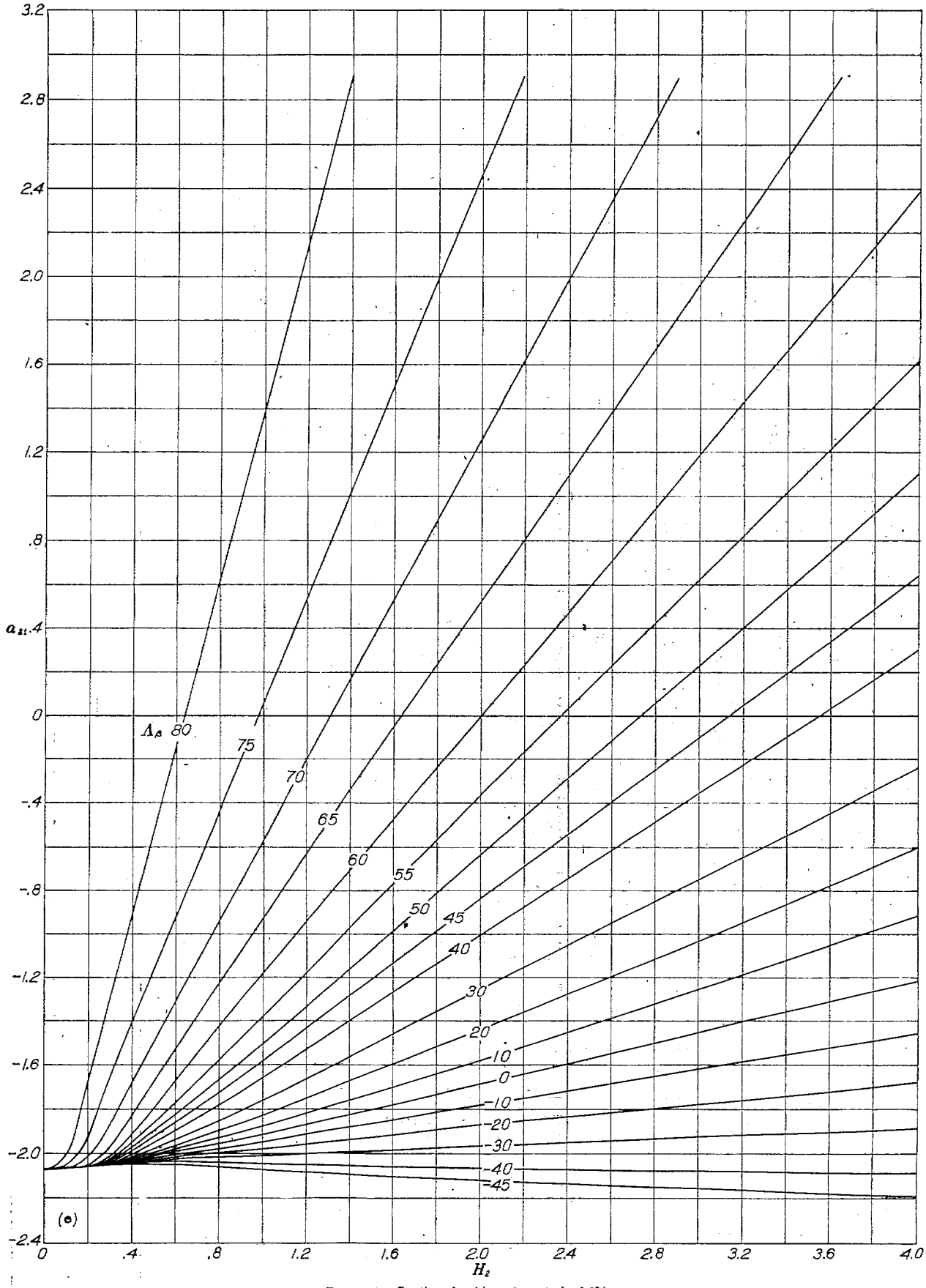

FIGURE 1.—Continued. (e) $\nu=2$, $n=1$, $d_1=0.234$.

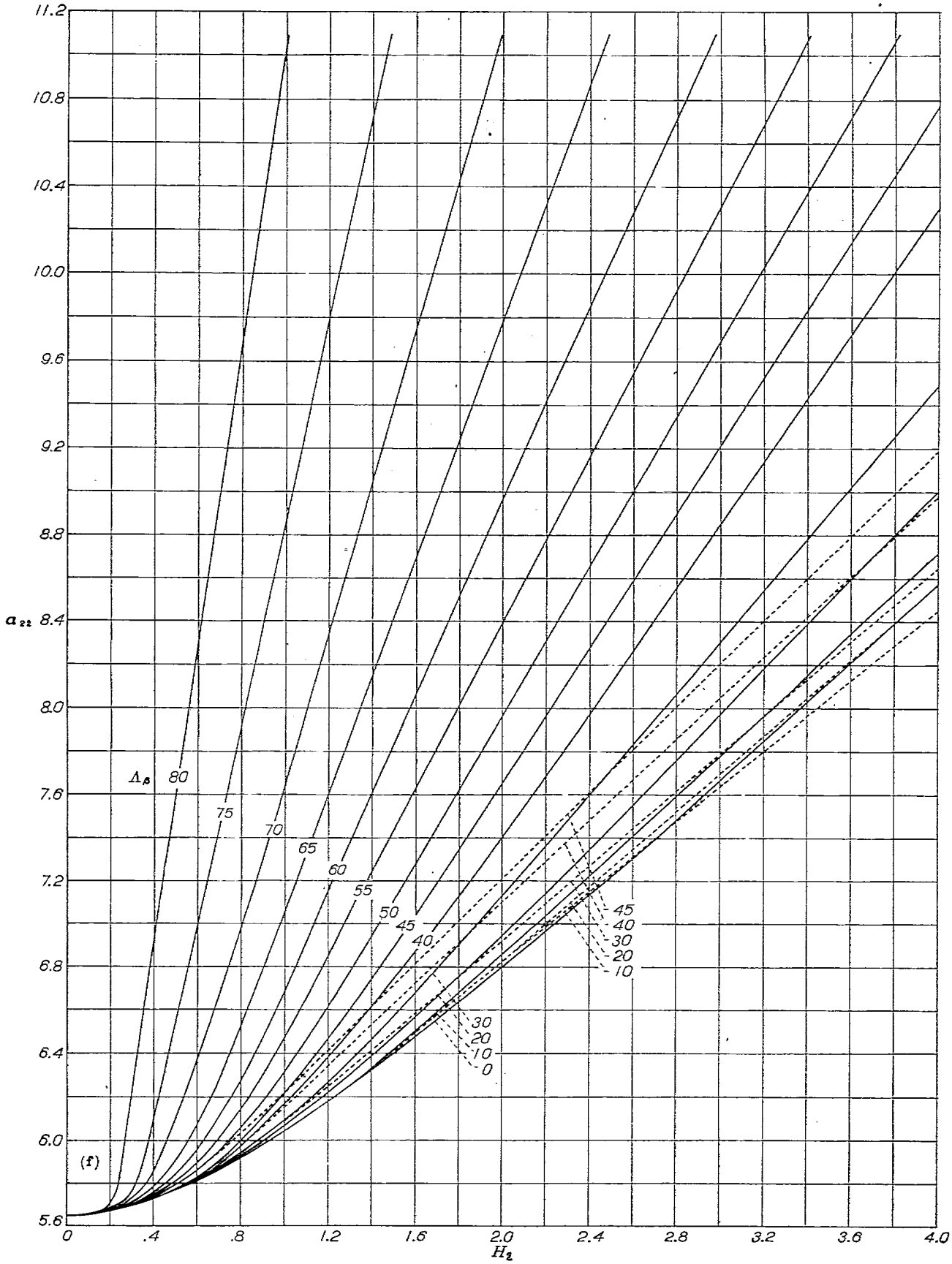

FIGURE 1.—Continued. (f) $\nu=2$, $n=2$, $d_1=0.234$.

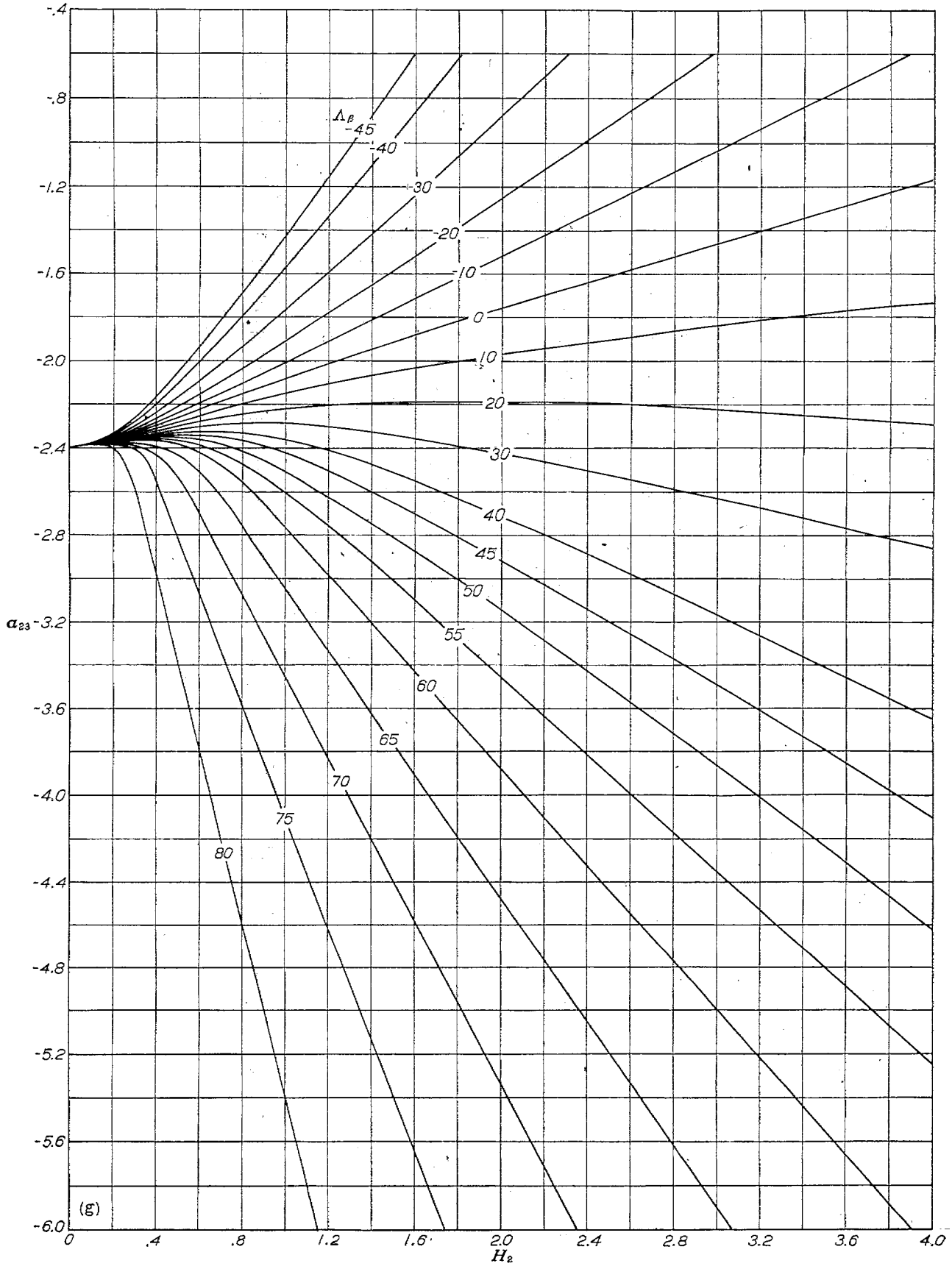

FIGURE 1.—Continued. (g) $\nu=2$, $n=3$, $d_1=0.234$.

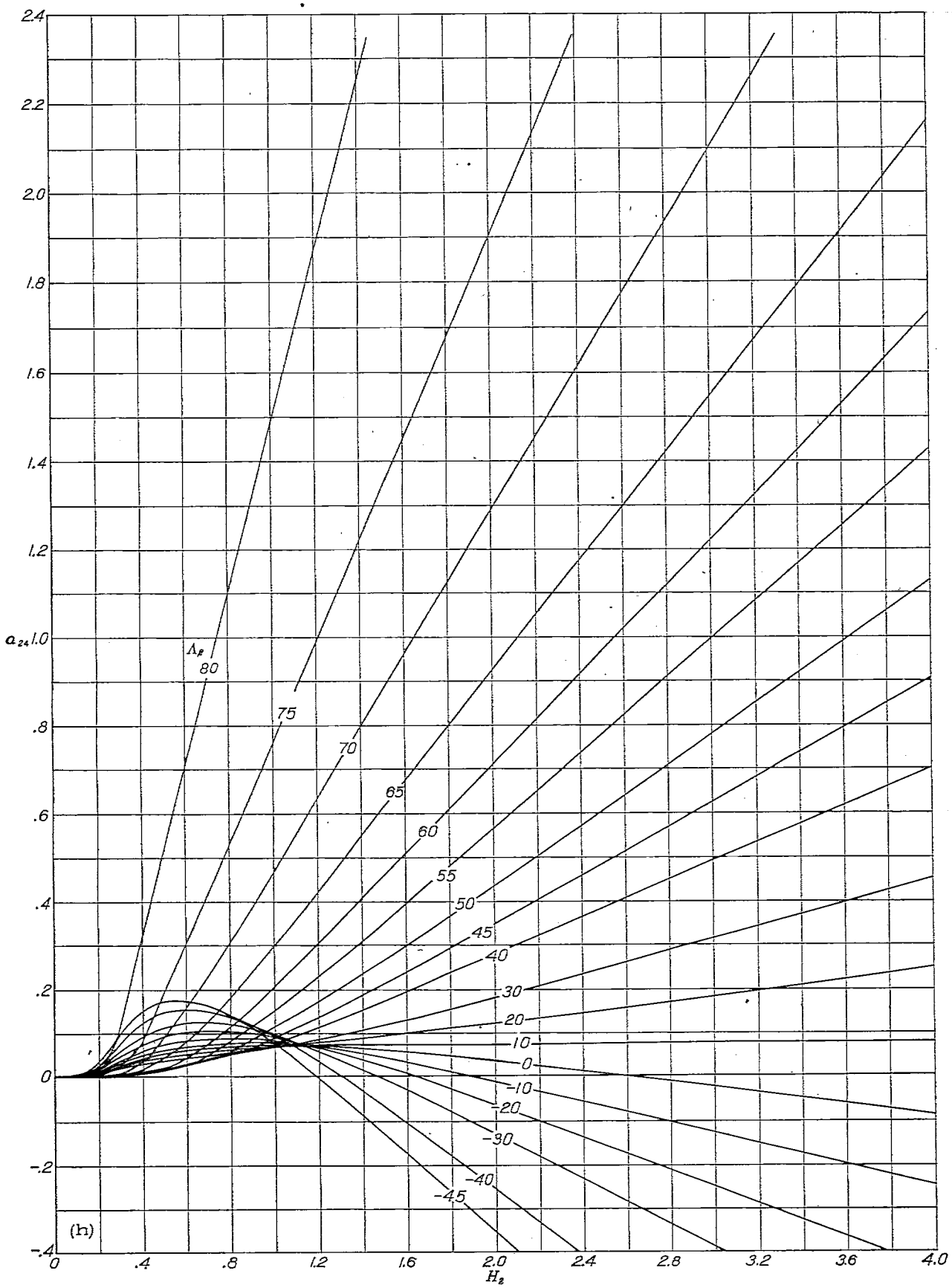

FIGURE 1.—Continued. (h) $\nu=2$, $n=4$, $d_2=0.234$.

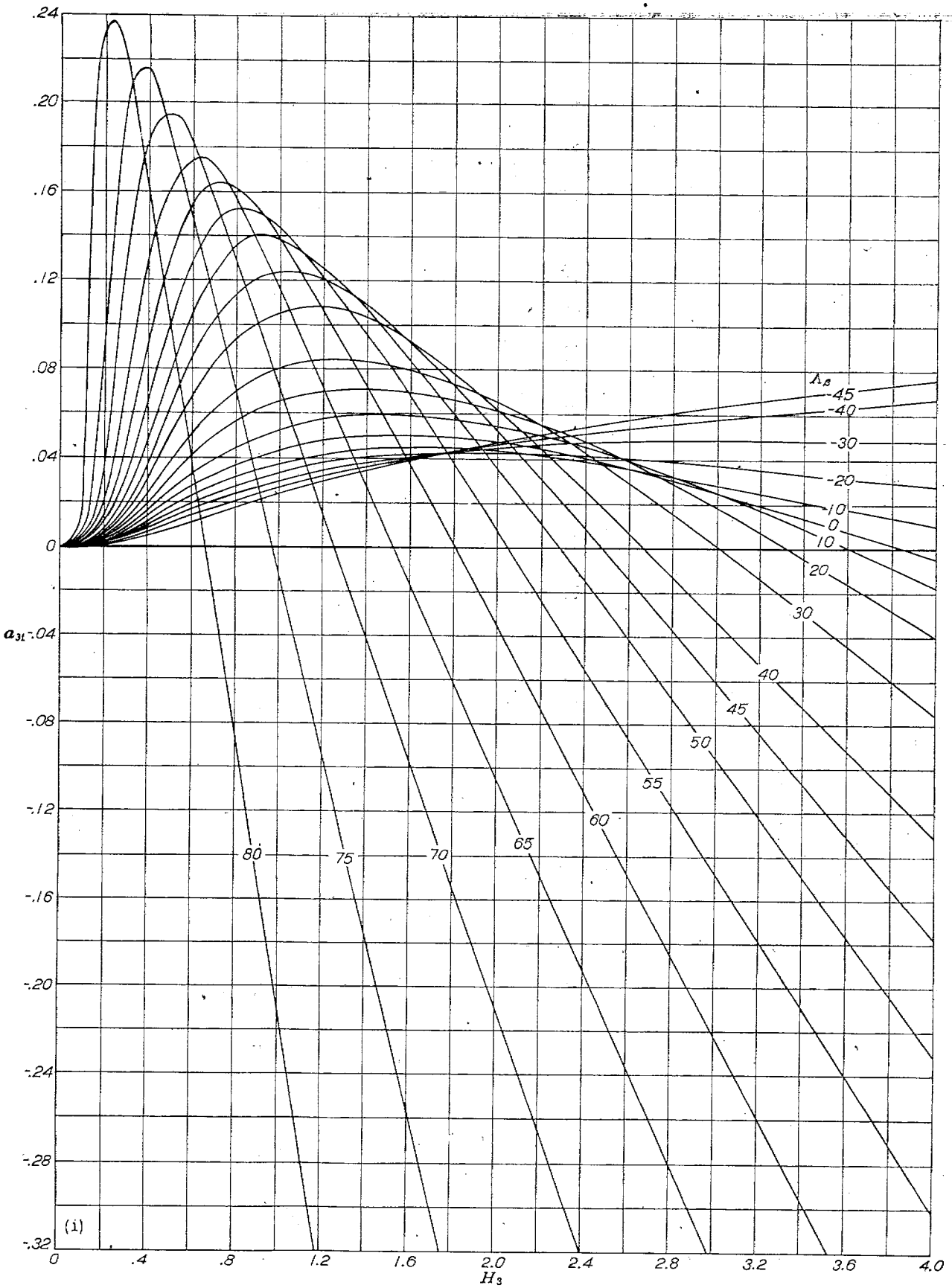

FIGURE 1.—Continued. (i) $\nu=3$, $n=1$, $d_3=0.381$.

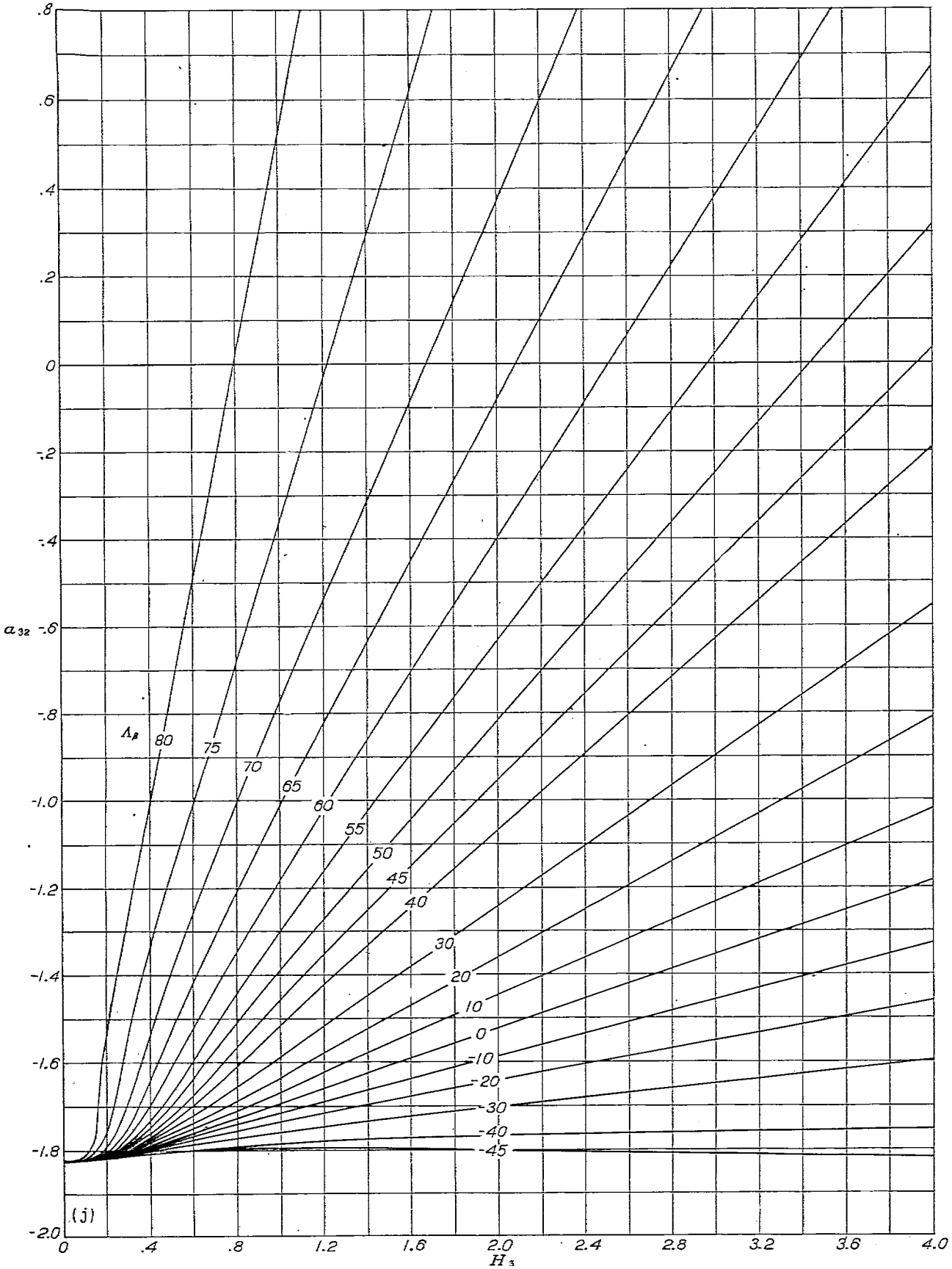

FIGURE 1.—Continued. (j) $\nu=3$, $n=2$, $d_3=0.381$.

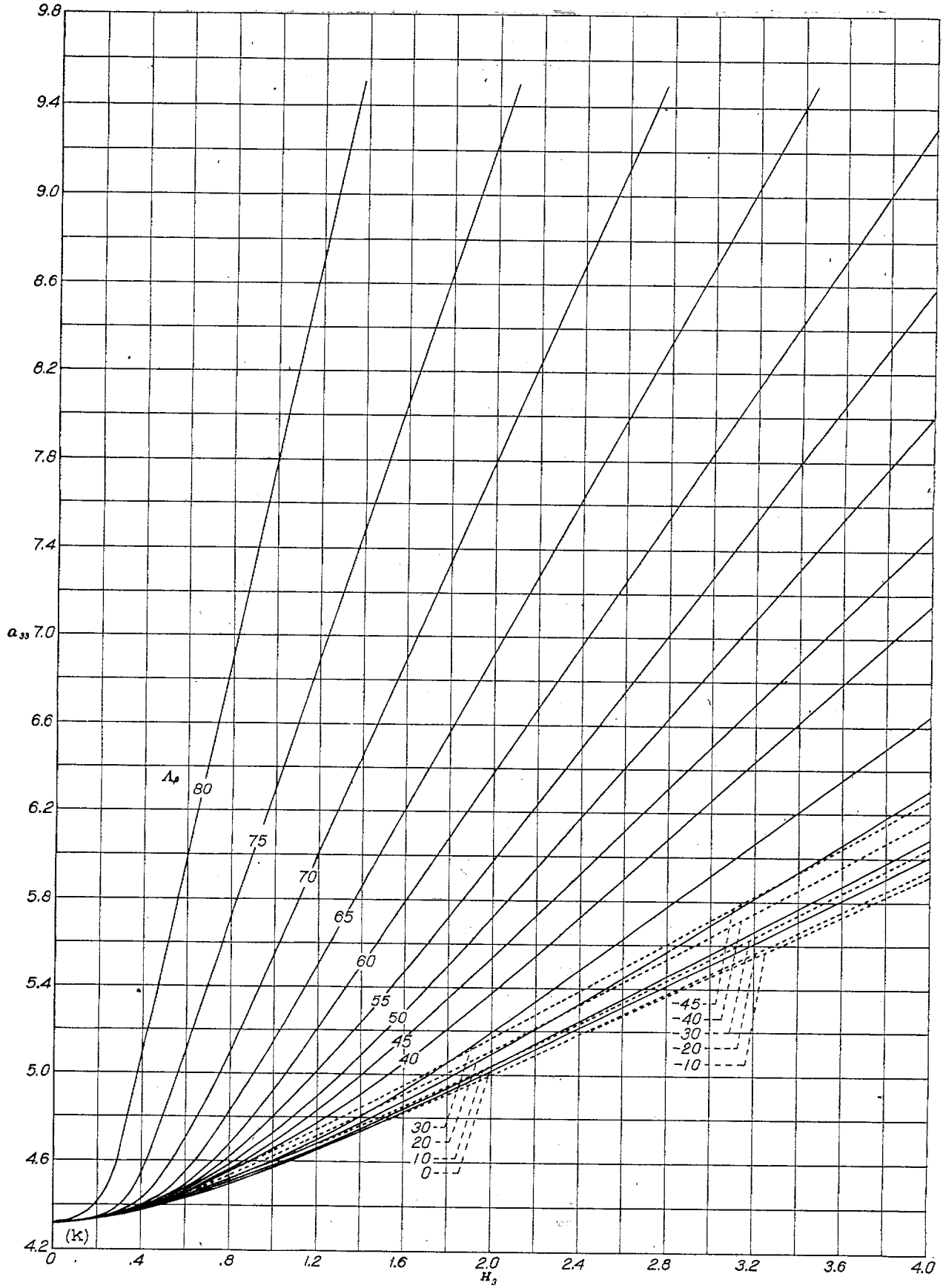

FIGURE 1.—Continued. (k) $\nu=3$, $n=3$, $d_2=0.381$.

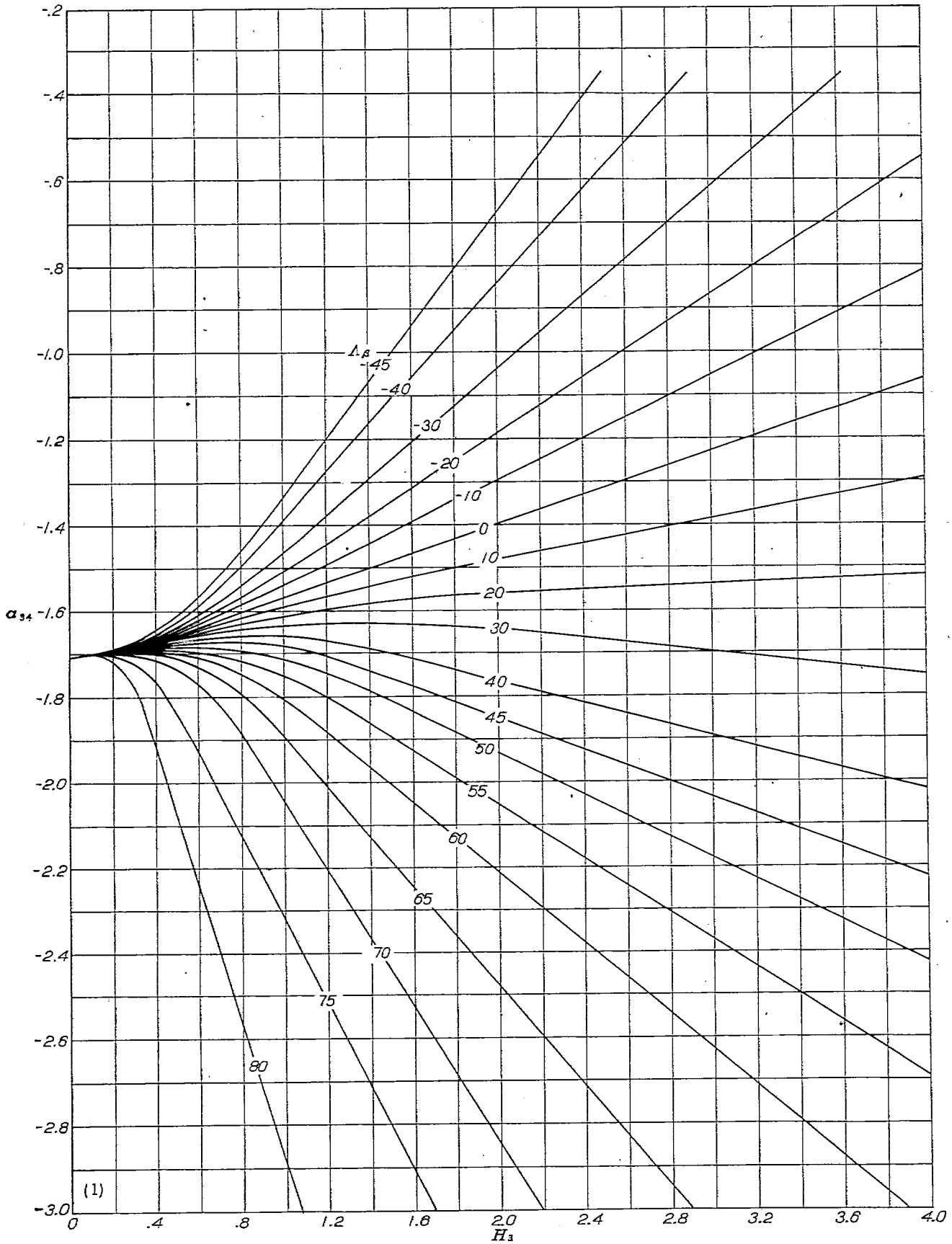

FIGURE 1.—Continued. (l) $\nu=3$, $n=4$, $d_3=0.381$.

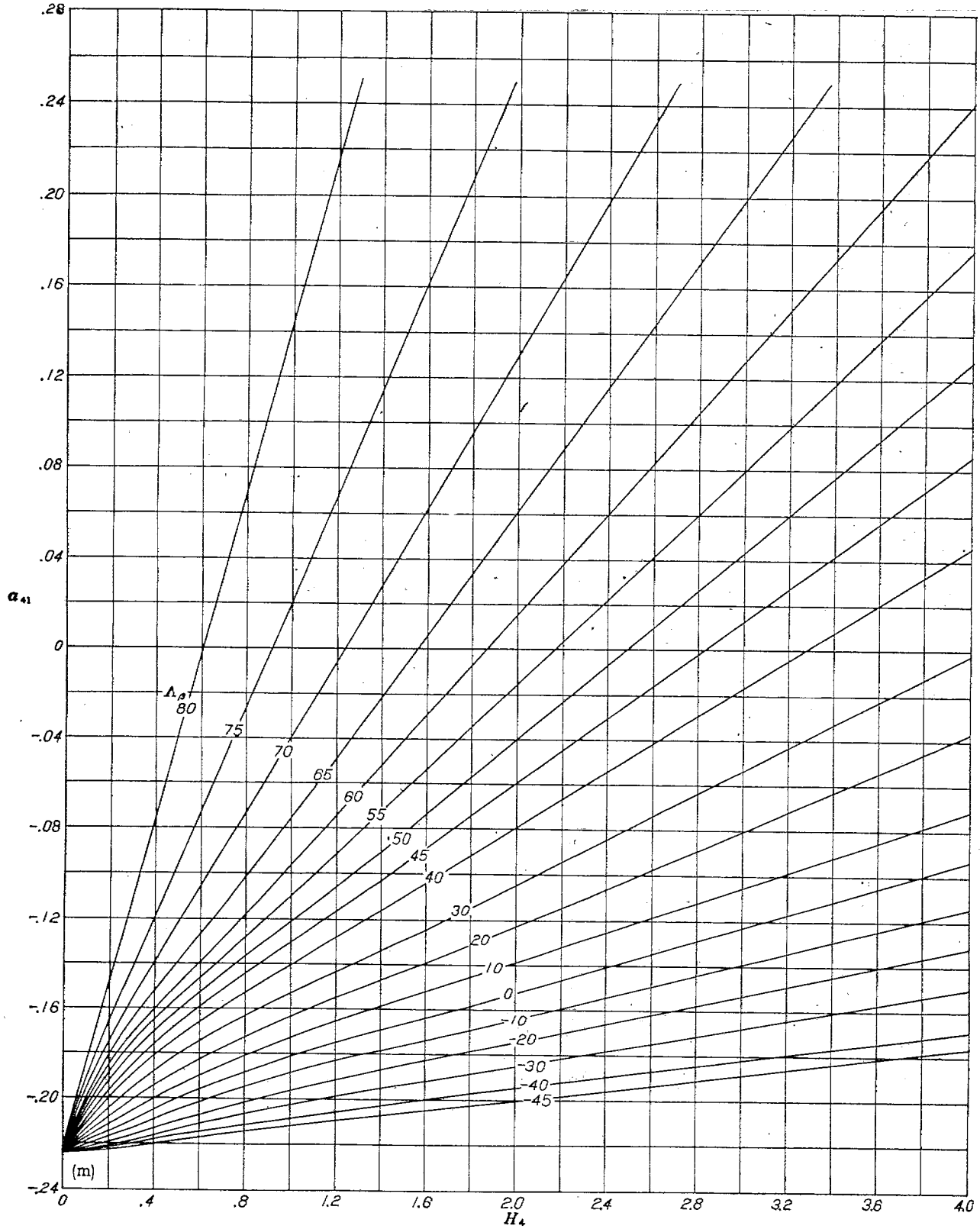

FIGURE 1.—Continued. (m) $\nu=4$, $n=1$, $d_4=0.320$.

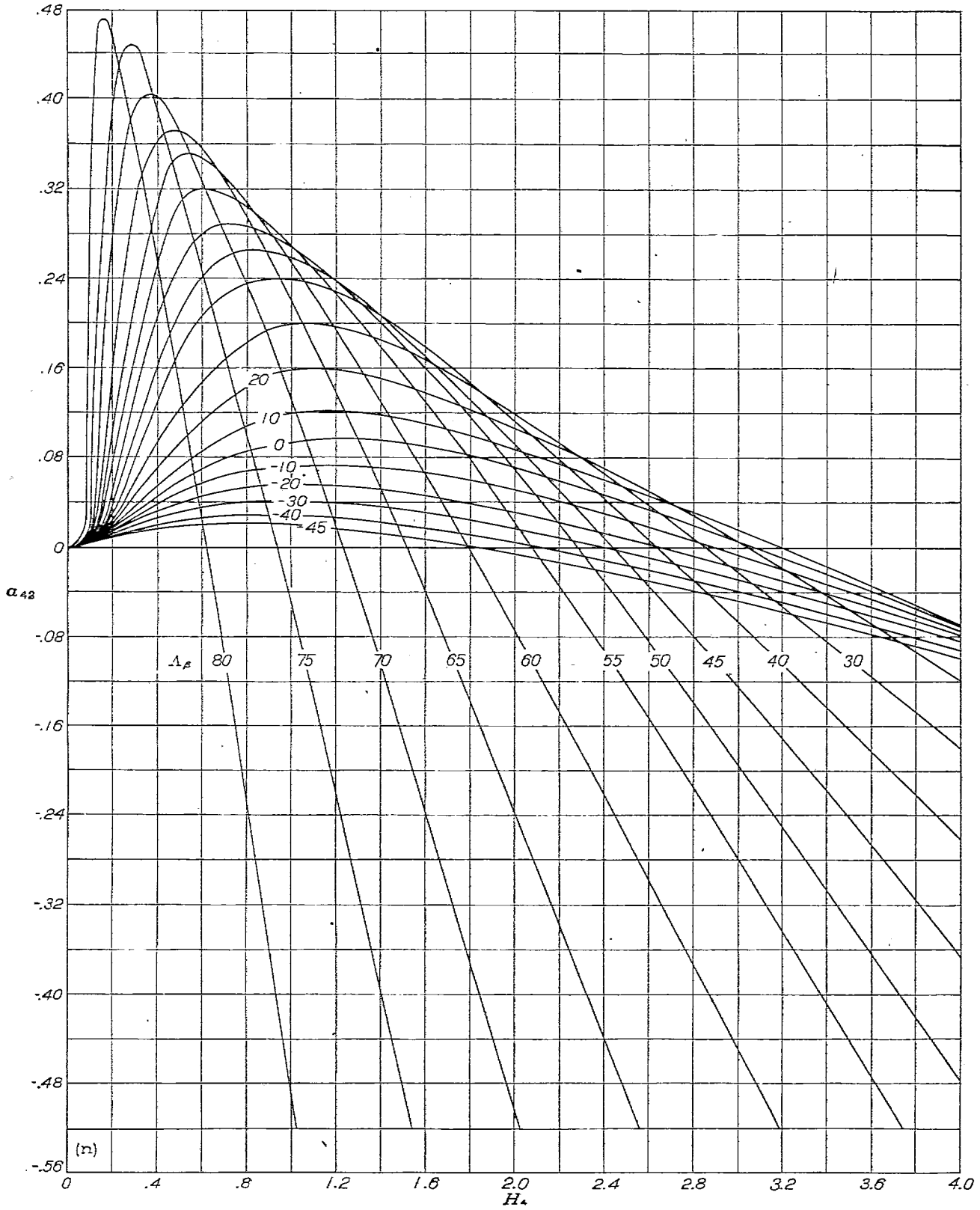

FIGURE 1.—Continued. (n) $\nu=4$, $n=2$, $d_4=0.320$.

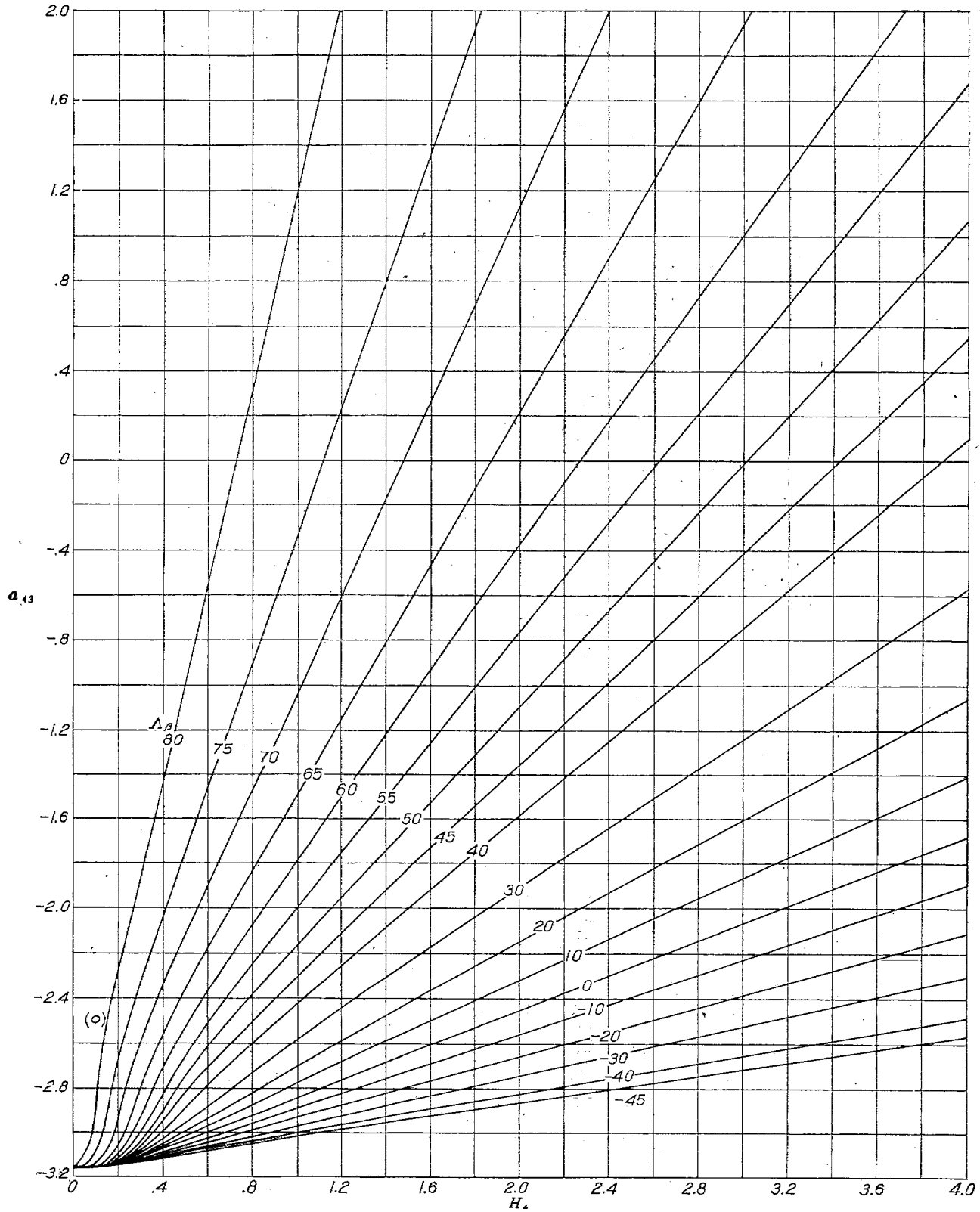

FIGURE 1.—Continued. (o) $\nu=4$, $n=3$, $d_4=0.320$.

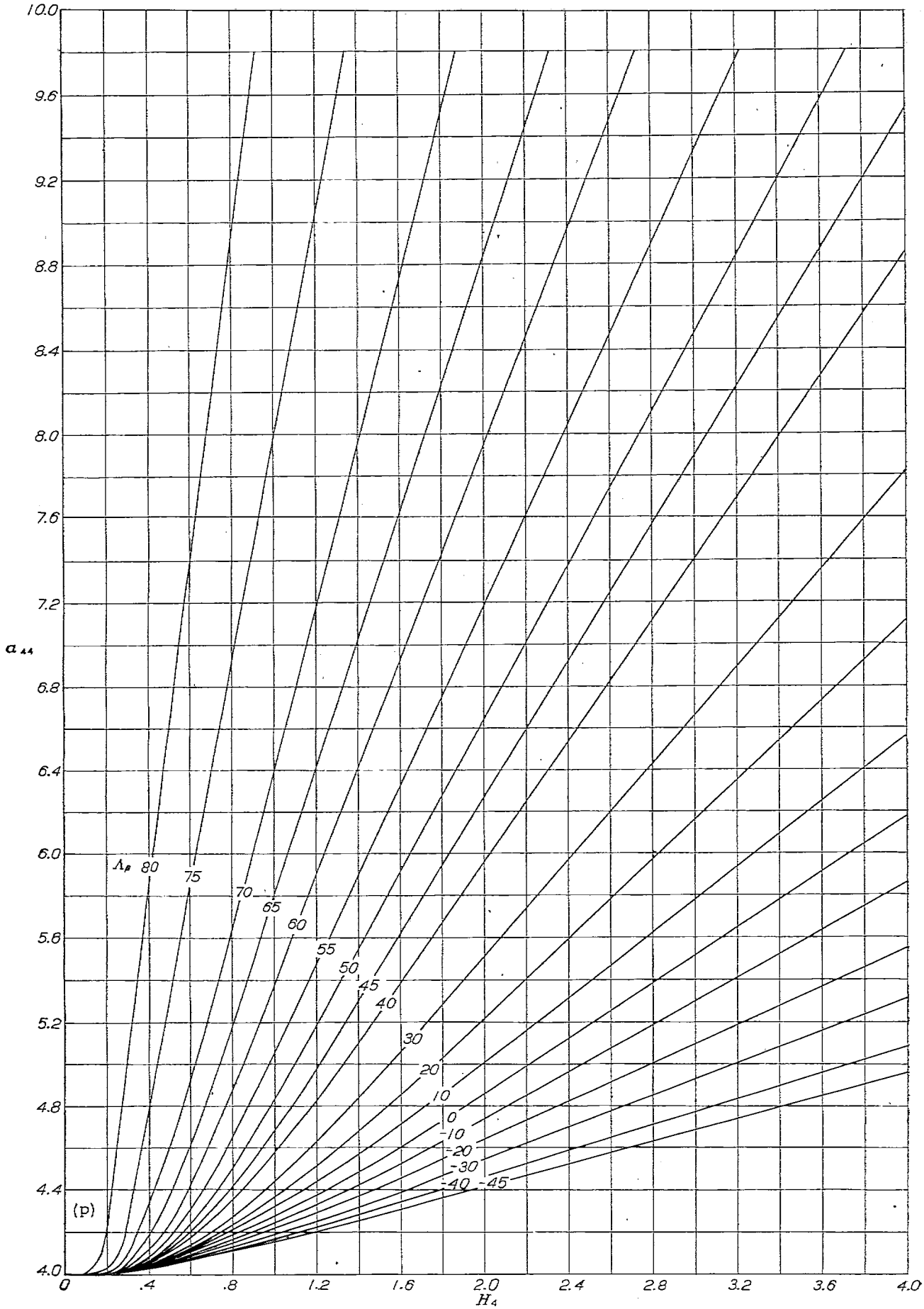

FIGURE 1.—Concluded. (p) $\nu=4$, $n=4$, $d_4=0.320$.

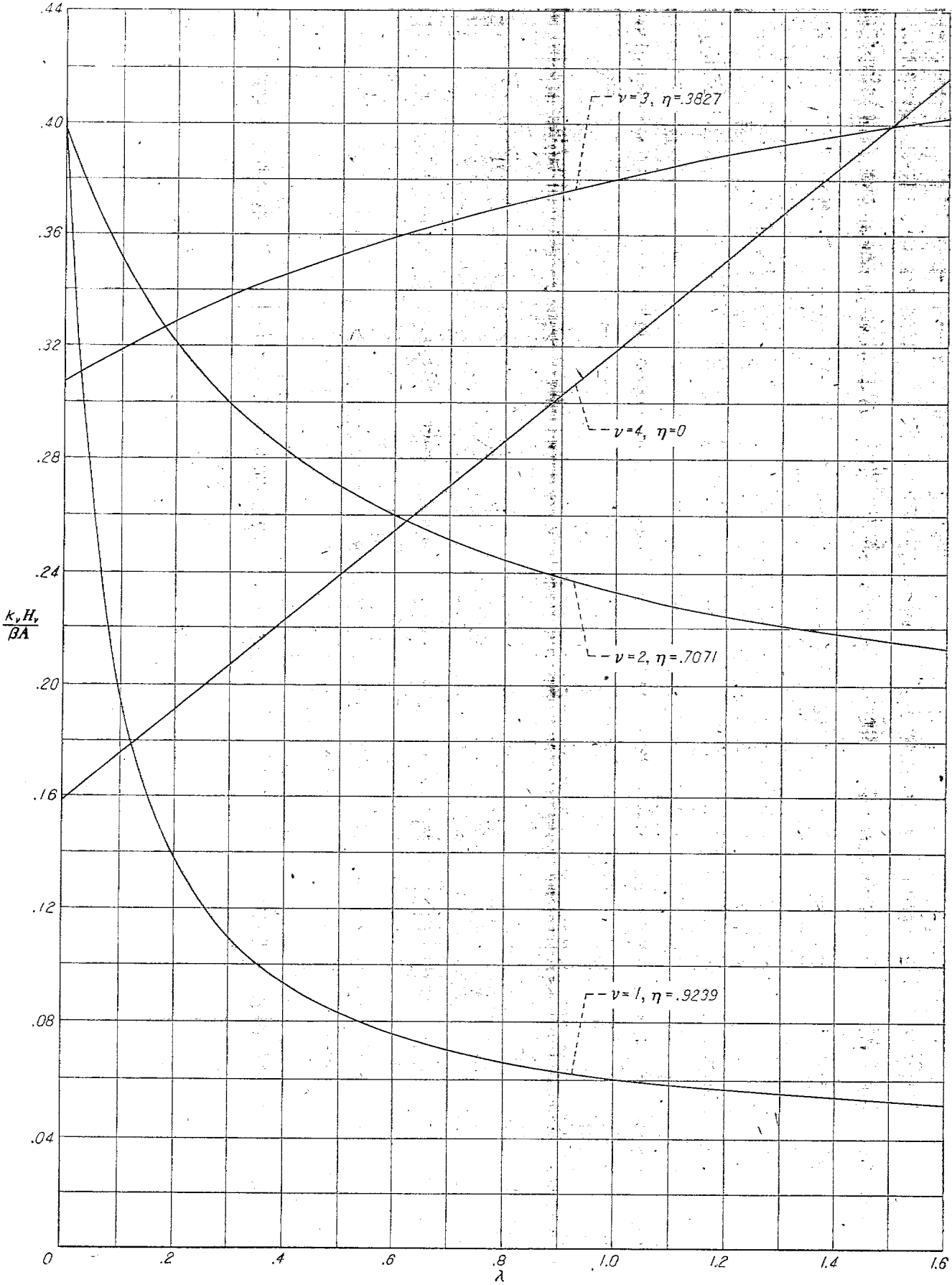

FIGURE 2.—Variation of the geometric parameter, $\frac{k_\nu H_\nu}{\beta A}$, with taper ratio, λ, for straight-tapered wings.

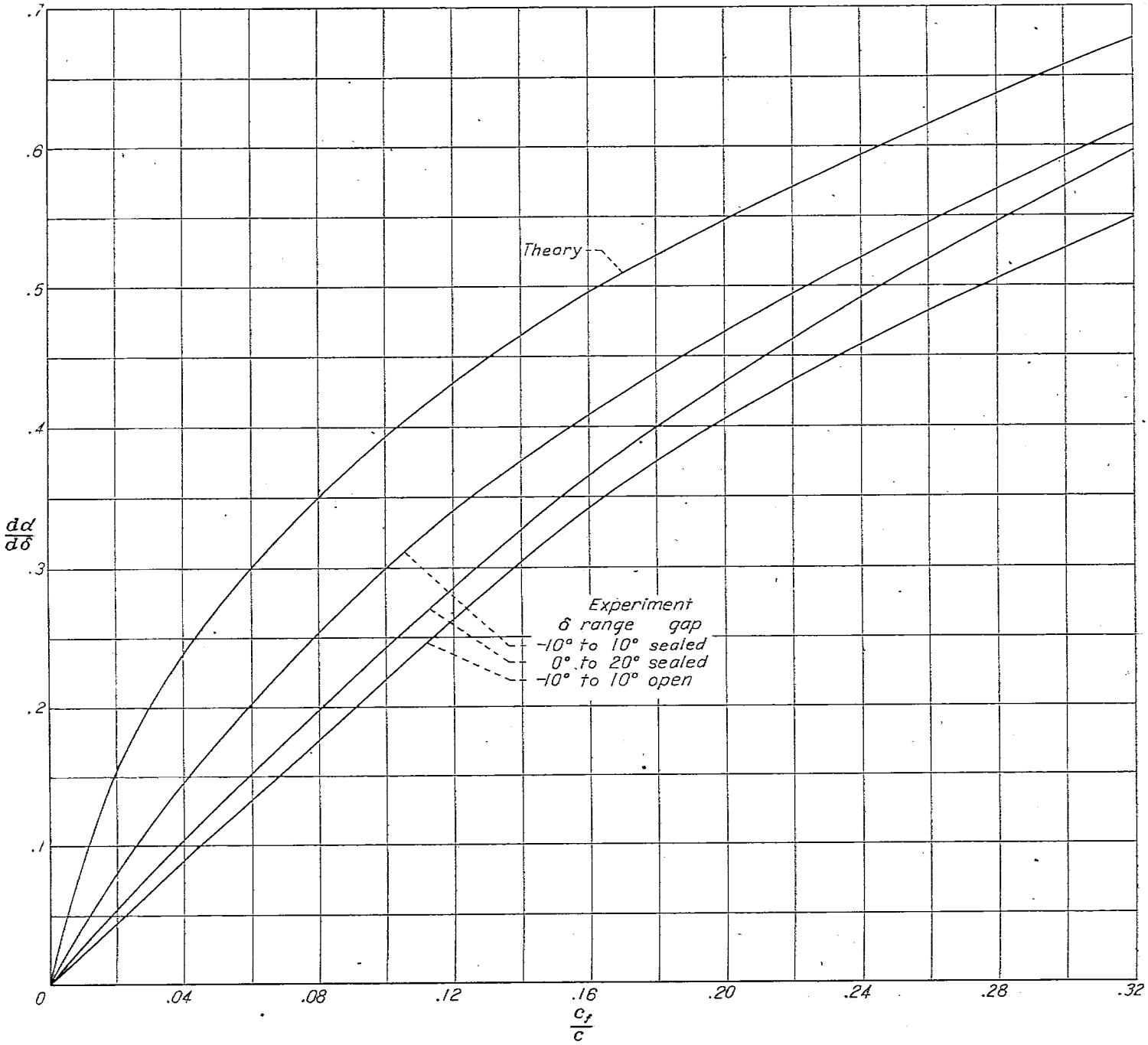

FIGURE 3.—Variation of lift-effectiveness parameter with flap-chord ratio, $\frac{c_f}{c}$. Average trailing-edge angle about 10°; $M=0.2$. (Curves from reference 4.)

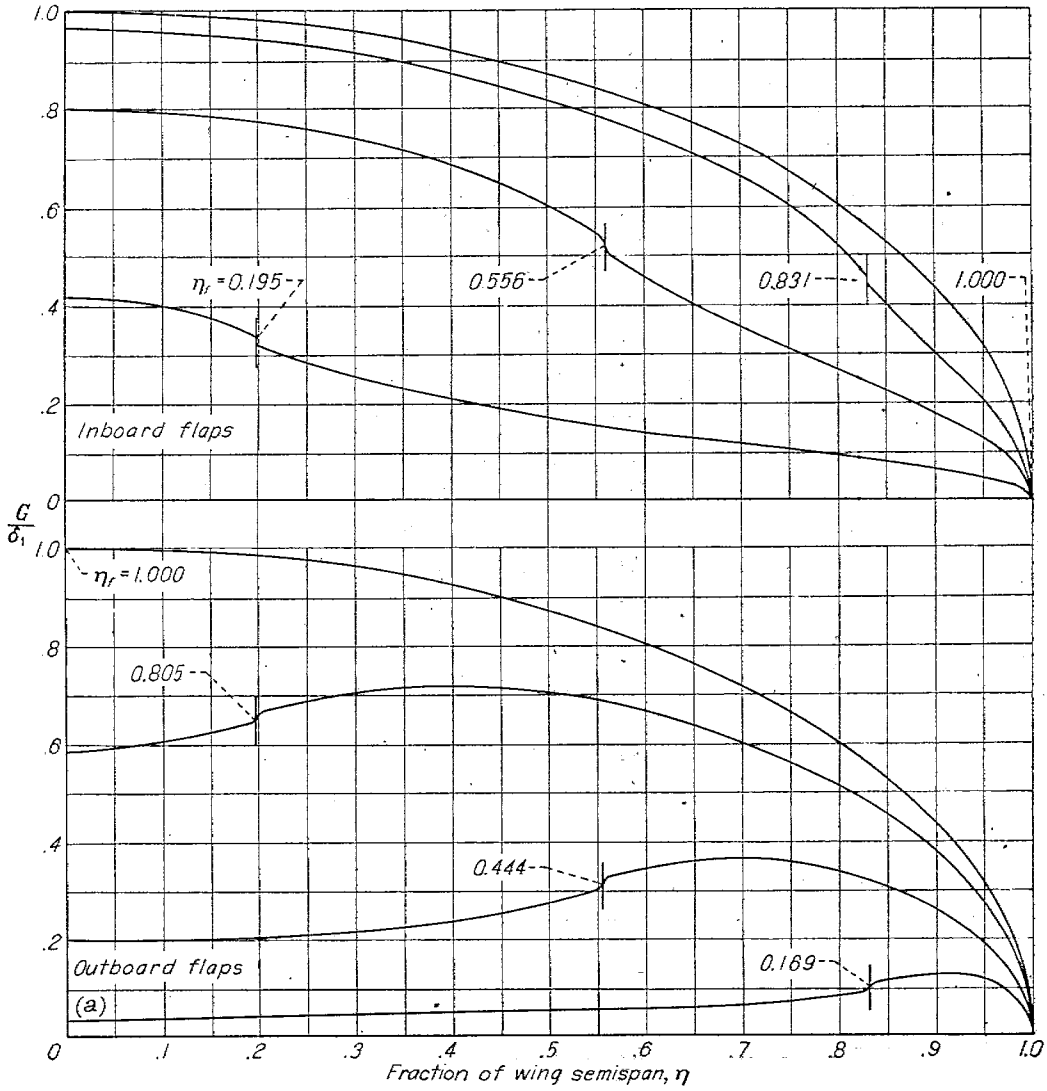

(a) $\frac{\beta A}{\kappa_{a_0}}=0$; inboard and outboard flaps for all plan forms with the trailing edge at or behind the upstream line of maximum span (reference 3).

FIGURE 4.—Spanwise load distribution, $\frac{G}{\delta_1}$, per radian, due to symmetric flap deflection for straight-tapered wings. $\frac{c_f}{c}=1$.

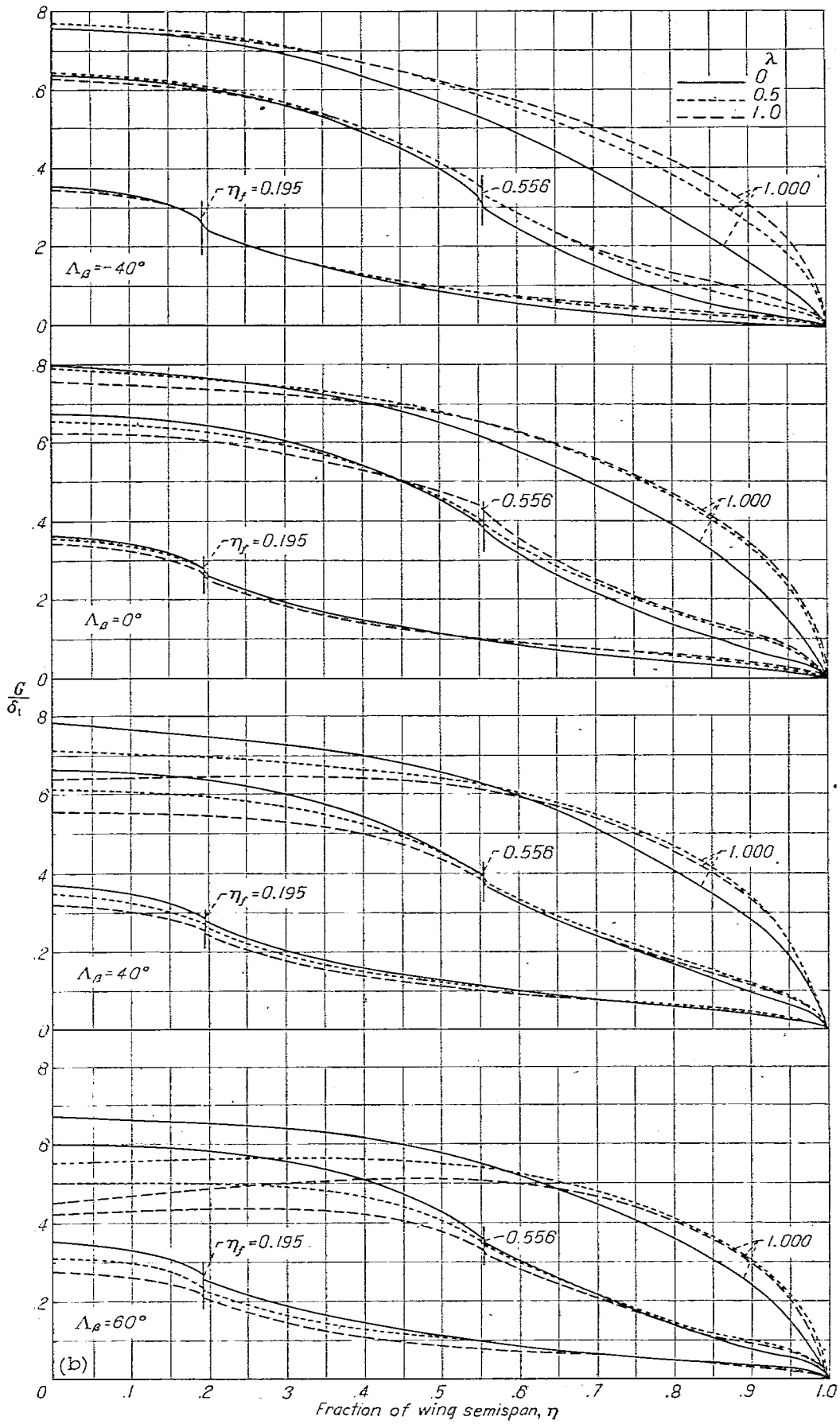

(b) $\frac{\beta A}{\kappa_{at}}$=2.0; inboard flaps.

FIGURE 4.—Continued.

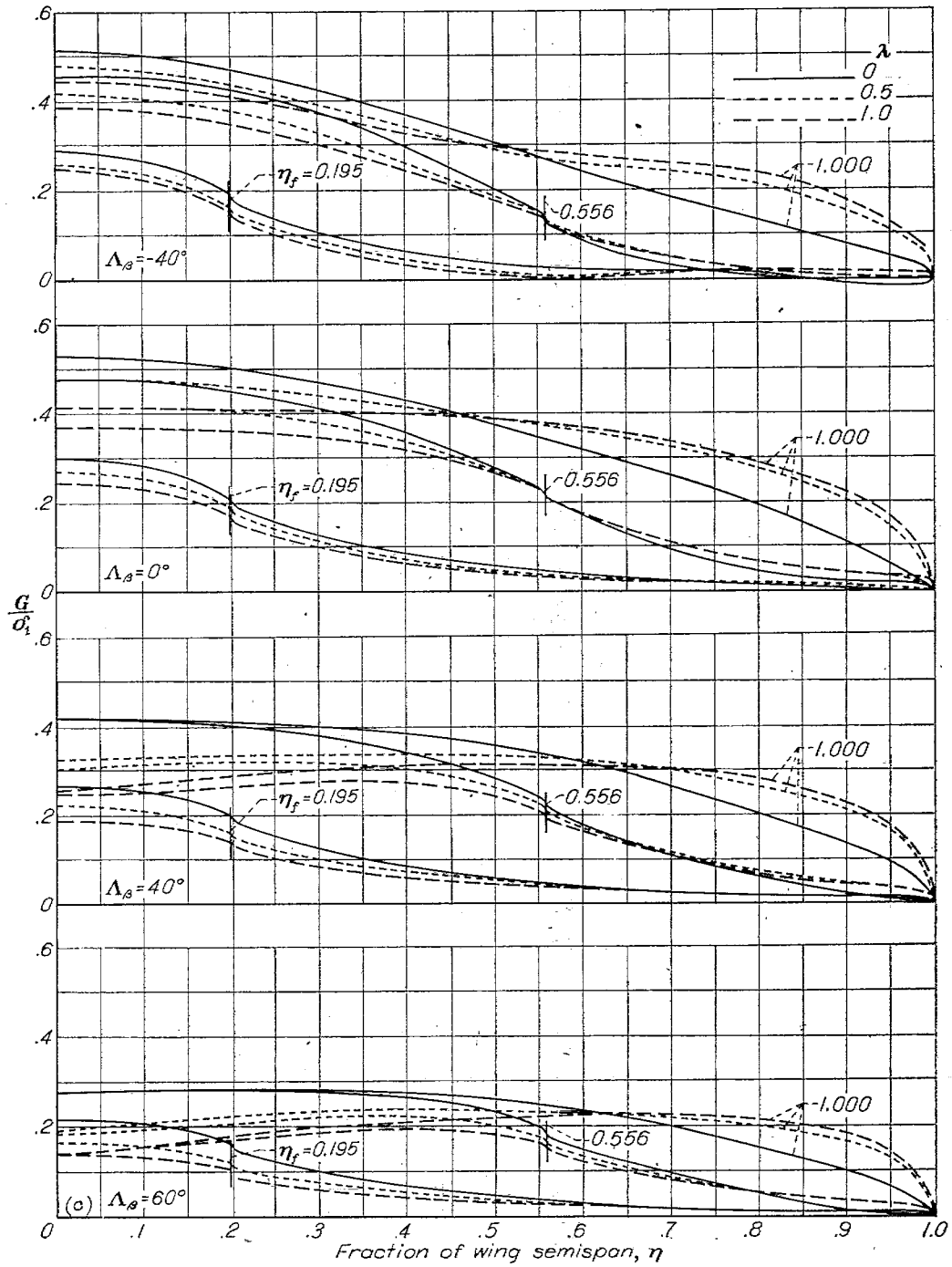

(c) $\frac{\beta A}{\kappa_{ag}}$=6.0; inboard flaps.

FIGURE 4.—Continued.

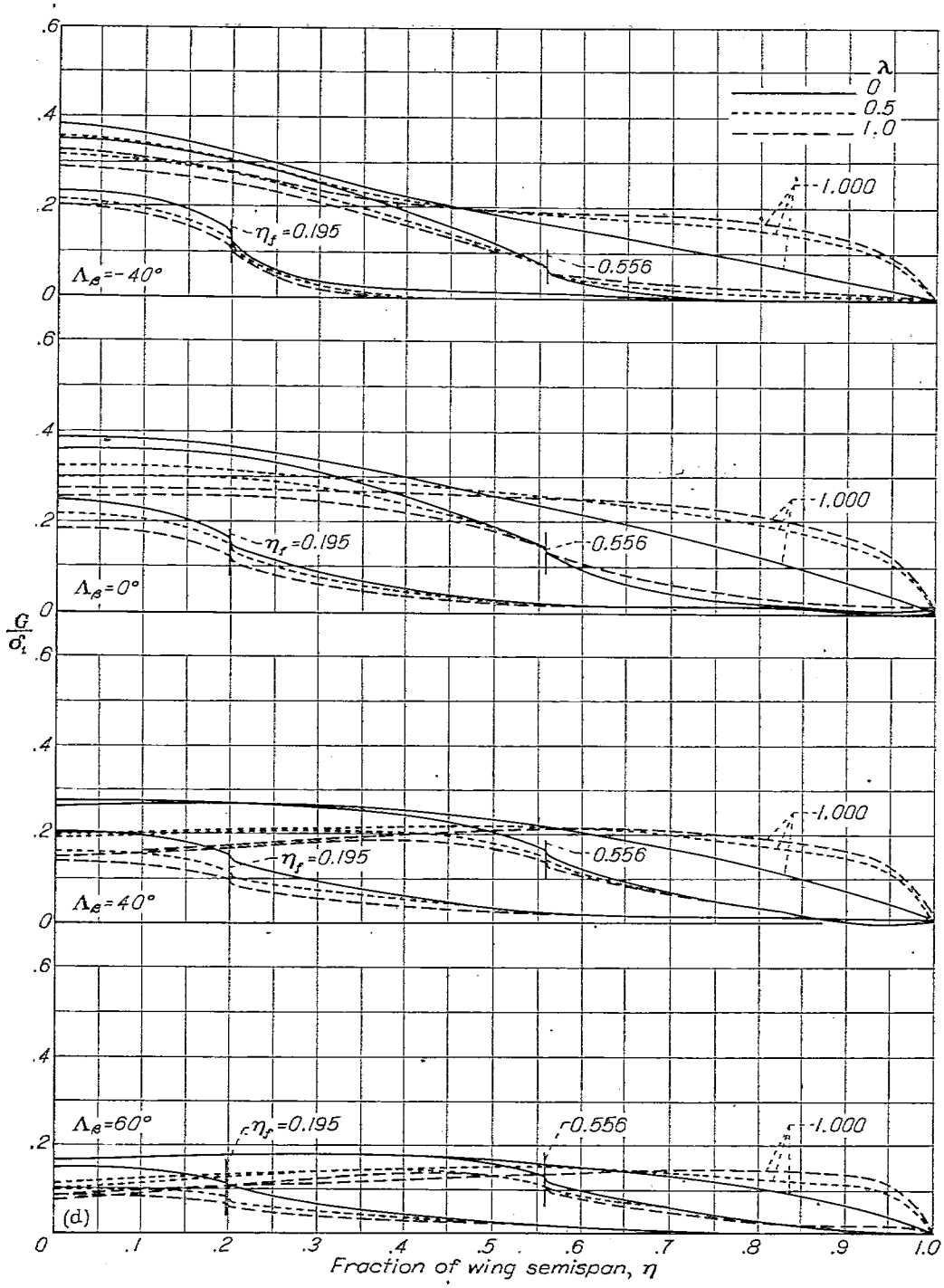

(d) $\frac{\beta A}{\kappa_{ss}}$=10.0; inboard flaps.

FIGURE 4.—Concluded.

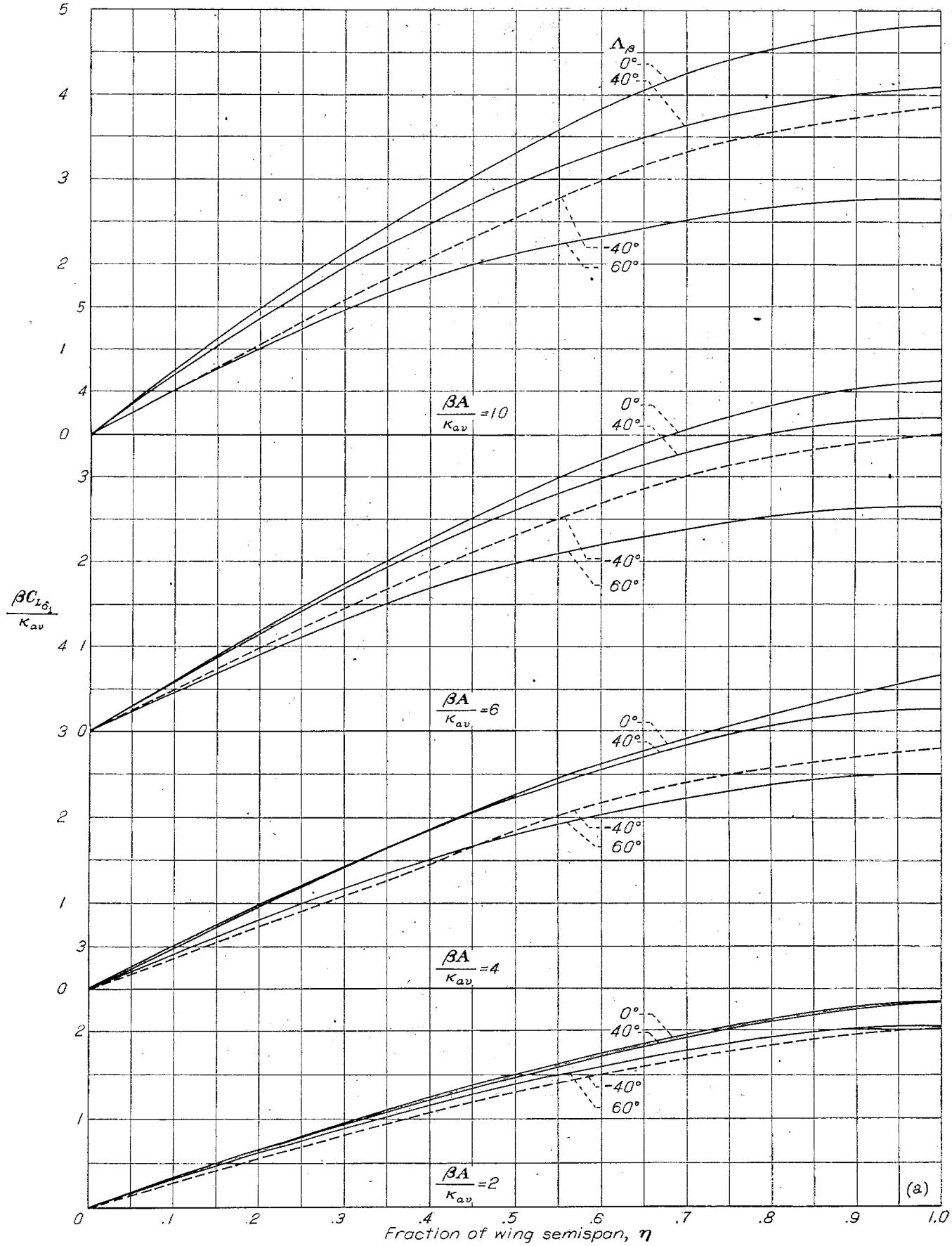

(a) λ=0.

FIGURE 5.—Flap lift parameter, $\frac{\beta C_{l\delta_1}}{\kappa_{av}}$ per radian, for extent of flap span from the wing root outboard, $\frac{c_f}{c}=1$.

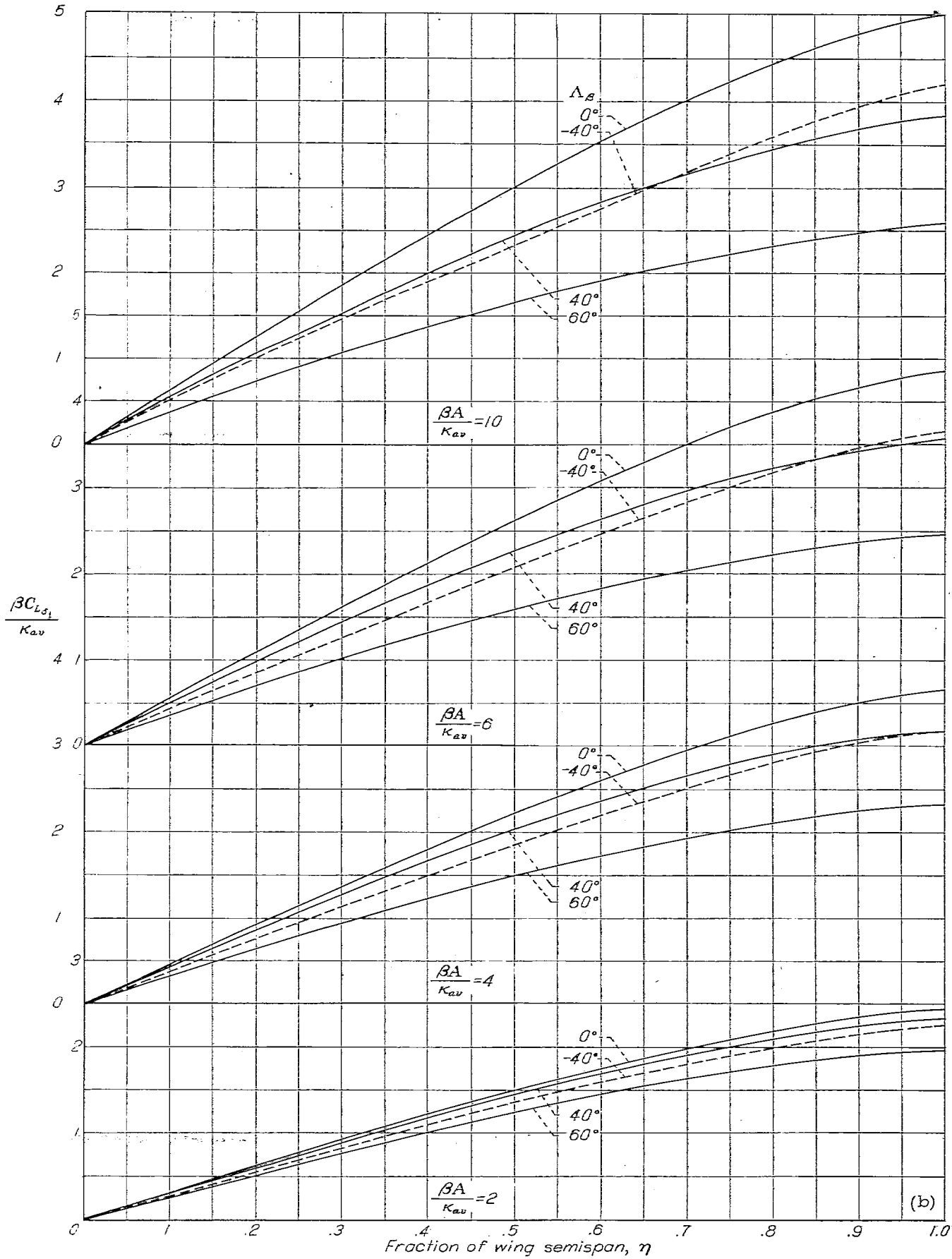

(b) λ=0.5.

FIGURE 5.—Continued.

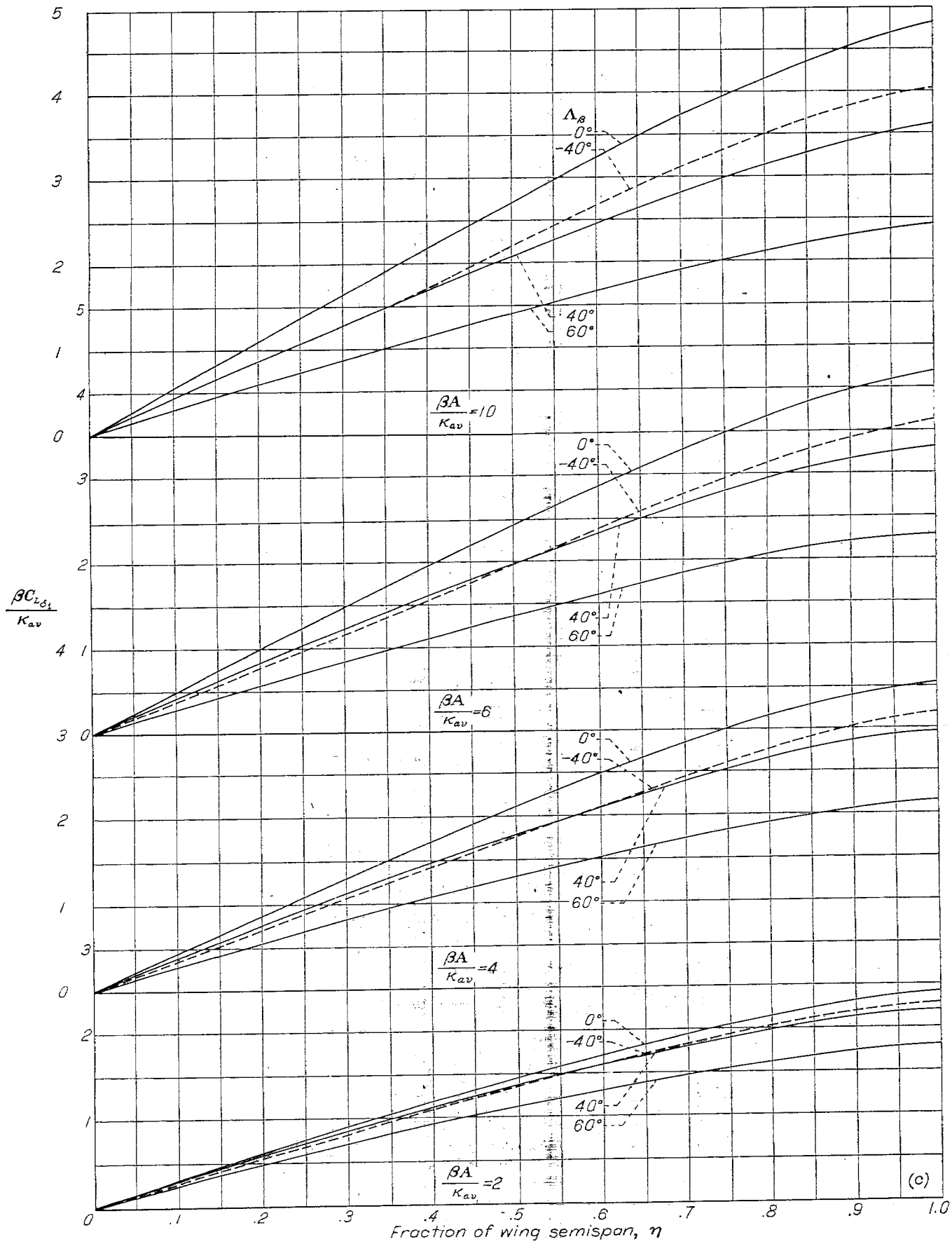

(c) λ=1.0.

FIGURE 5.—Concluded.

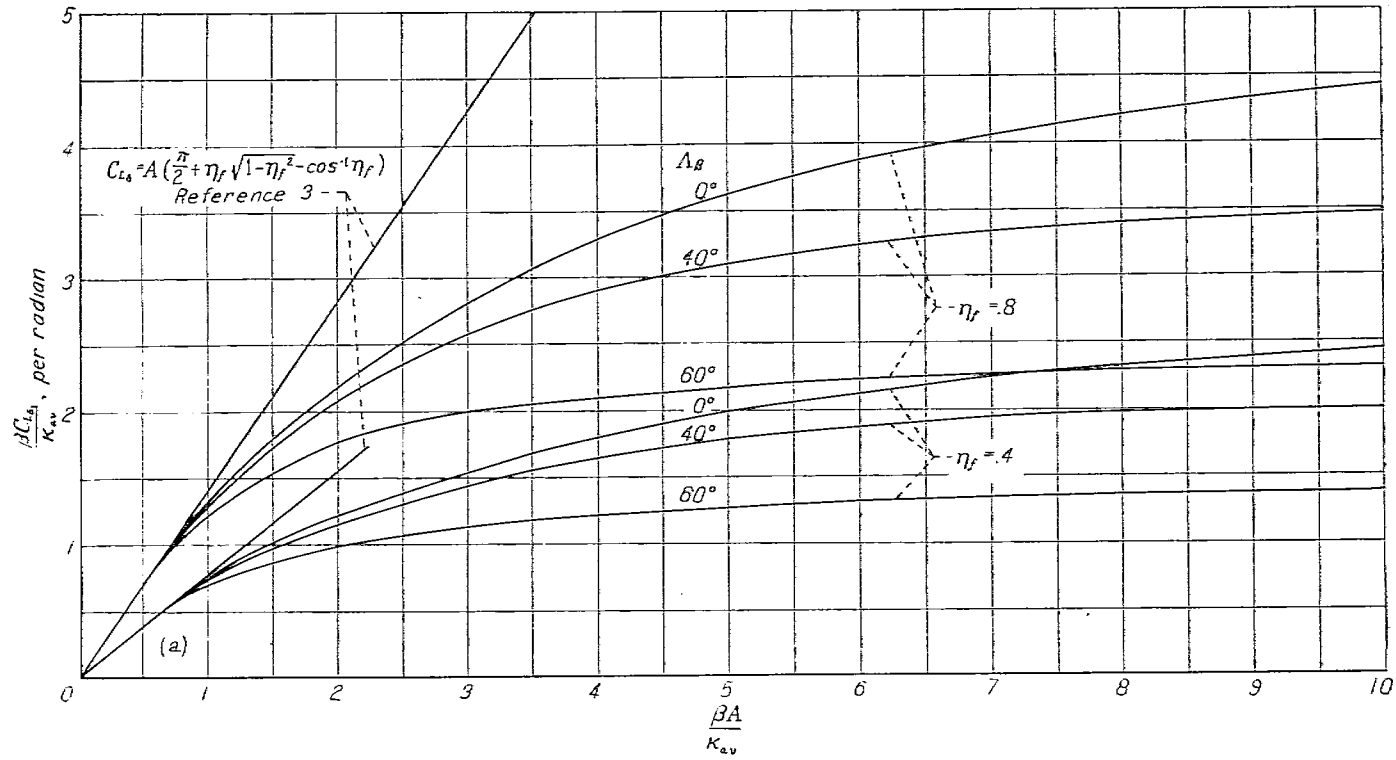

(a) Effect of aspect ratio for $\lambda = 0.5$.

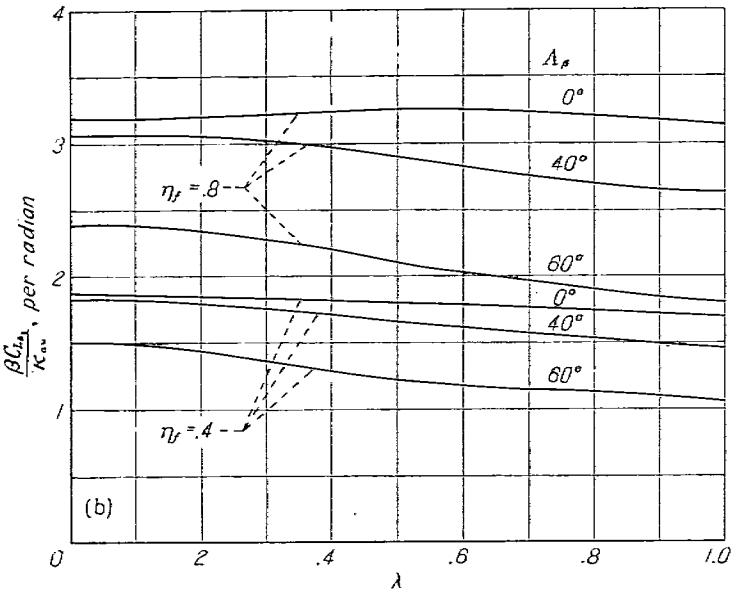

(b) Effect of taper ratio for $\frac{\beta A}{K_{av}} = 4.0$.

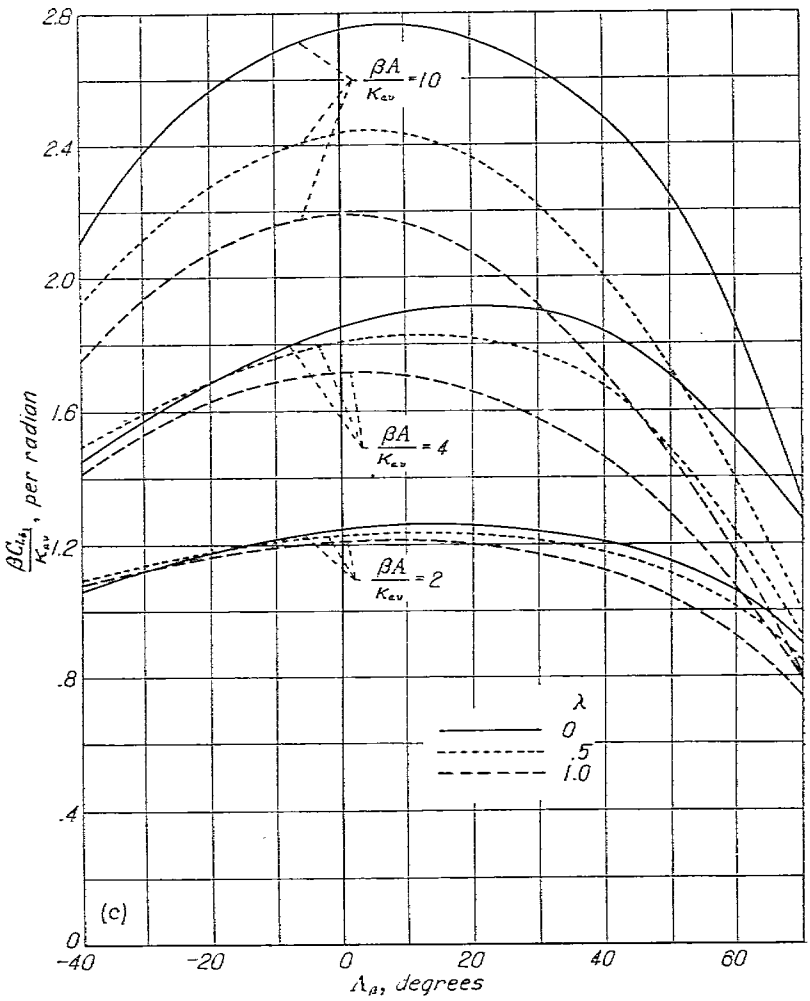

(c) Effective sweep for $\eta_f = 0.4$.

FIGURE 6.—Influence of wing geometry on flap effectiveness $\left(\frac{c_f}{c} = 1\right)$.

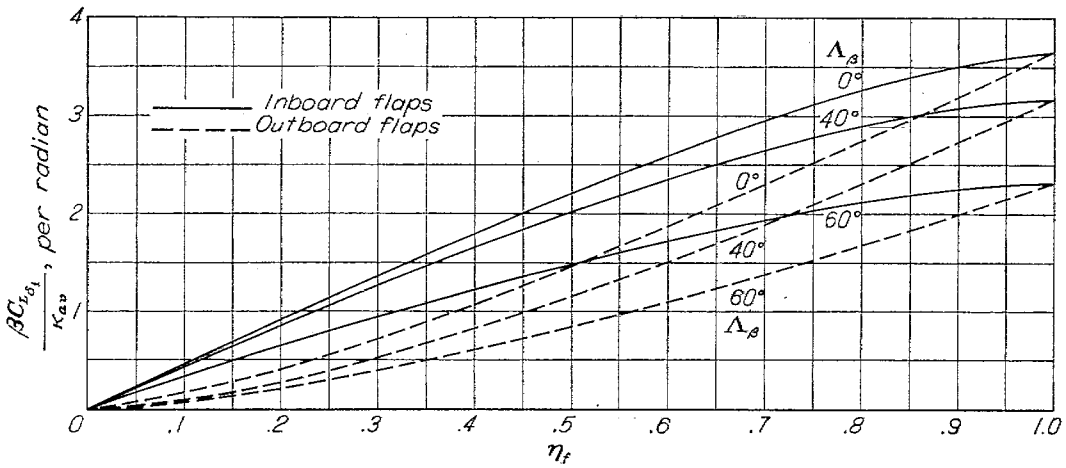

FIGURE 7.—Flap effectiveness as a function of flap span. $\frac{\beta A}{\kappa_{av}}=4$, $\lambda=0.5$, $\frac{c_f}{c}=1$.

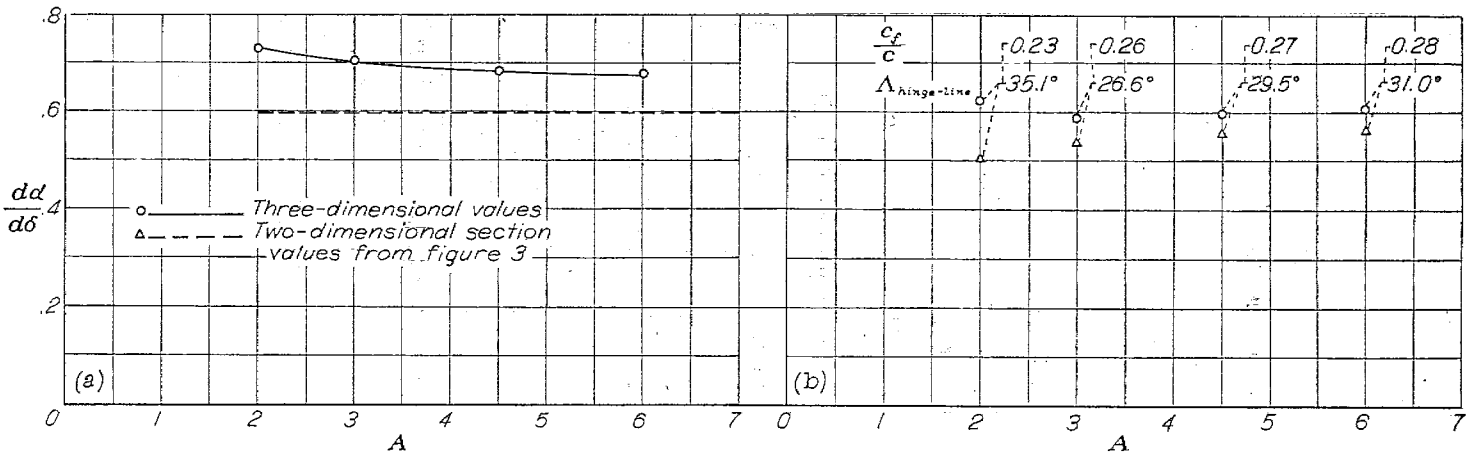

FIGURE 8.—Variation of experimentally determined $d\alpha/d\delta$ with aspect ratio for wings having flaps of 30 percent of the wing chord normal to the quarter-chord line. $\eta_f=1.0$, $\lambda=0.5$. (a) Unswept wing; $\Lambda_{\text{hinge line}}=0°$. (b) Swept wing.

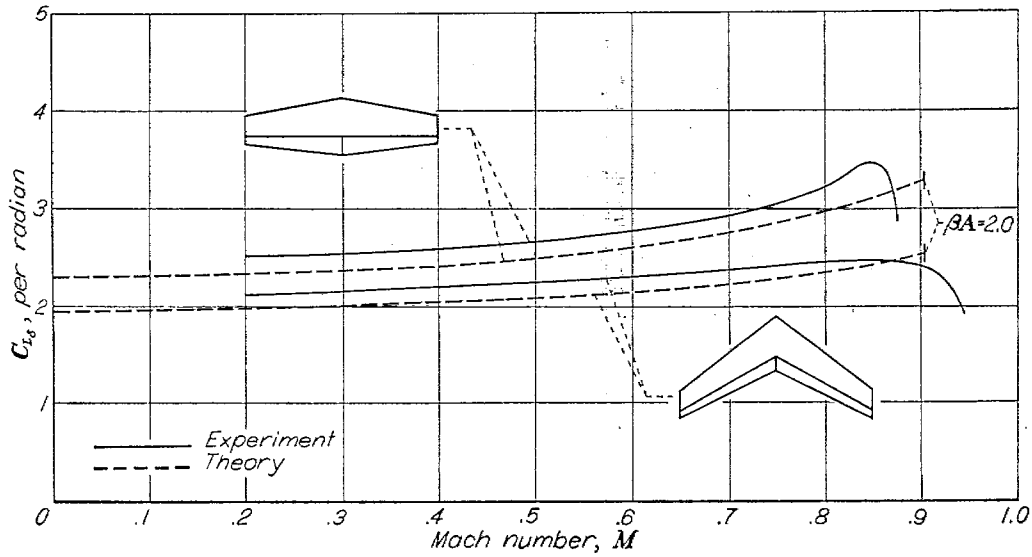

FIGURE 9.—Comparison of theoretical and experimental flap-effectiveness variation with Mach number. Reynolds number $\cong 2\times10^6$ at $M=0.2$; 4.8×10^6 at $M=0.6$.

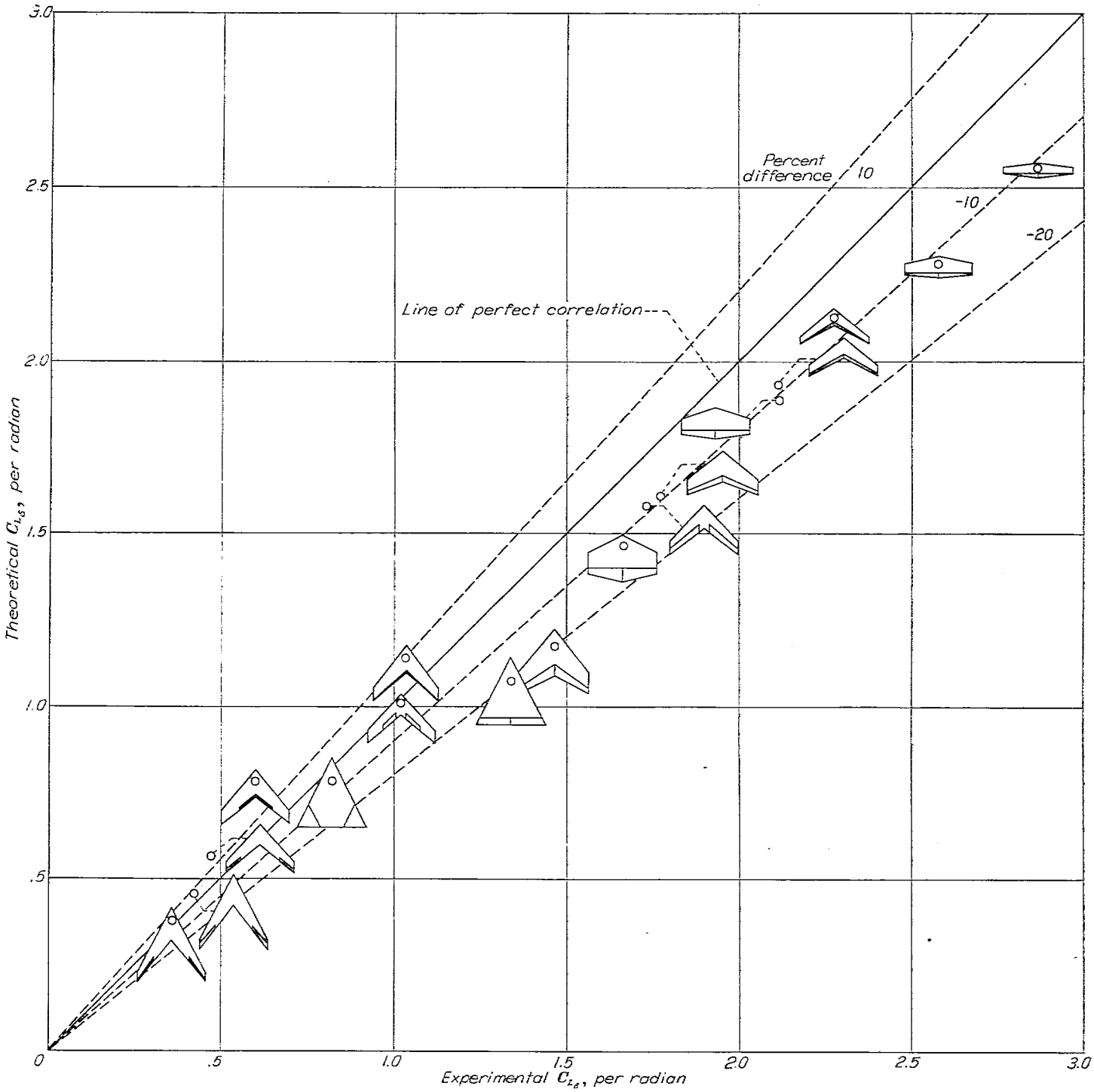

FIGURE 10.—Correlation of theoretical and low-speed experimental flap-effectiveness due to symmetrically deflected flaps for various plan forms. Reynolds number from 1 to 3×10⁶. $M<0.2$.